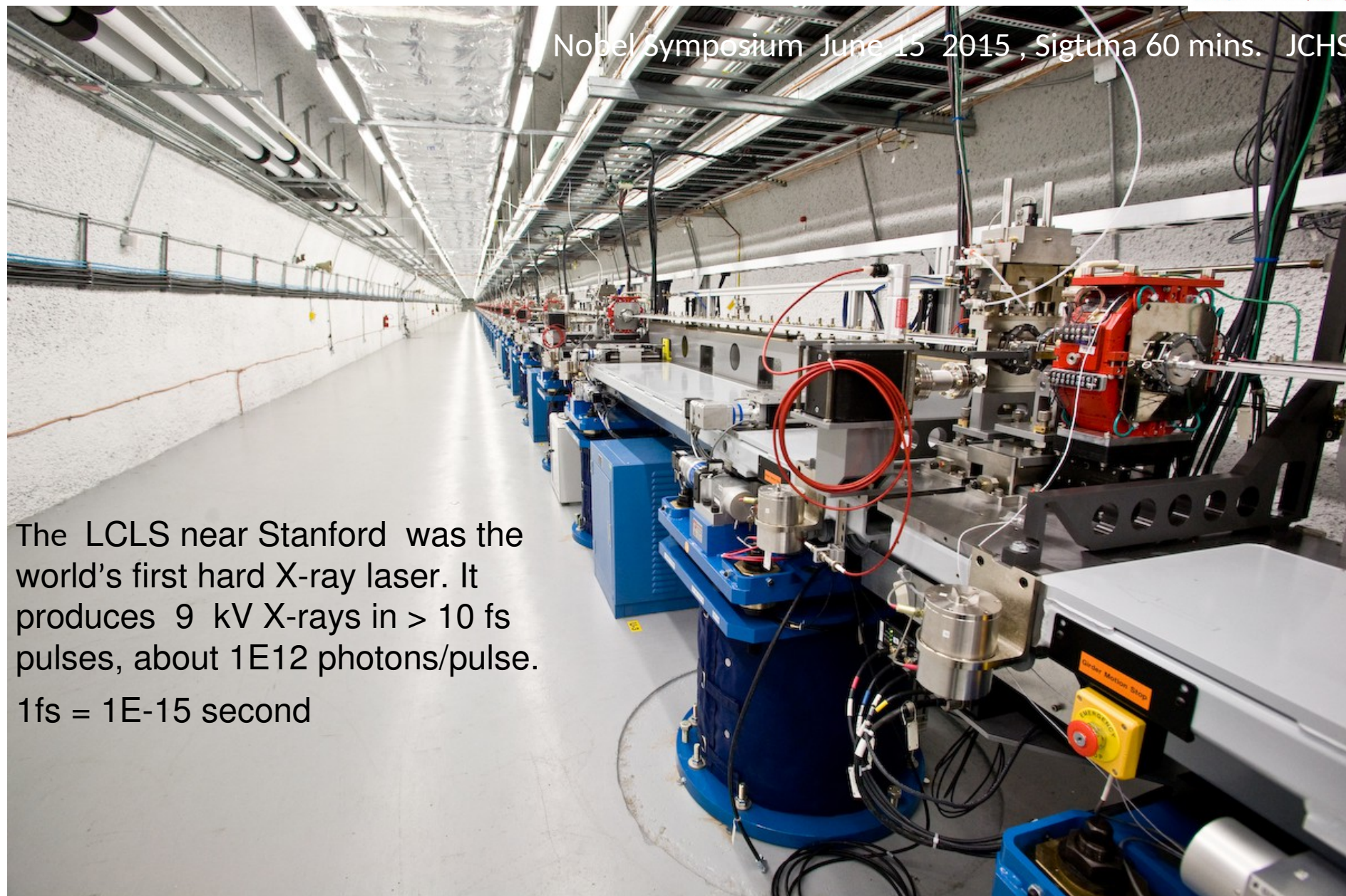


New approaches to biology using hard X-ray lasers

Nobel Symposium June 15 2015 , Sigtuna 60 mins. JCHS

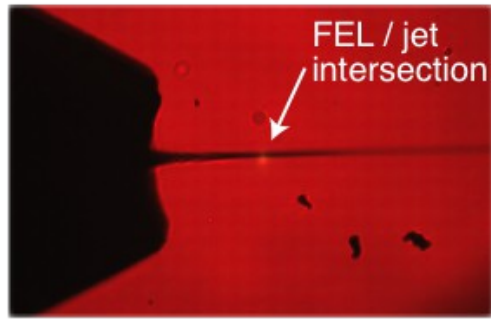


The LCLS near Stanford was the world's first hard X-ray laser. It produces 9 kV X-rays in > 10 fs pulses, about $1E12$ photons/pulse.

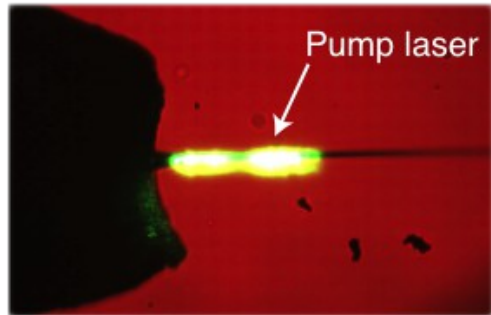
1fs = $1E-15$ second

Madey 1972 Stanford; Saldin, Bonifacio, Sessler 1985 Microwaves; Pellegrini optical 1991; Leutl 1997 Argonne; Flash Matterlink 1997 ; Murphy Brookhaven 2001; (SASE mode)

*Nanocrystals are sprayed across the pulsed X-ray beam.
This also allows Time-Resolved SFX (serial fs xtallog).*



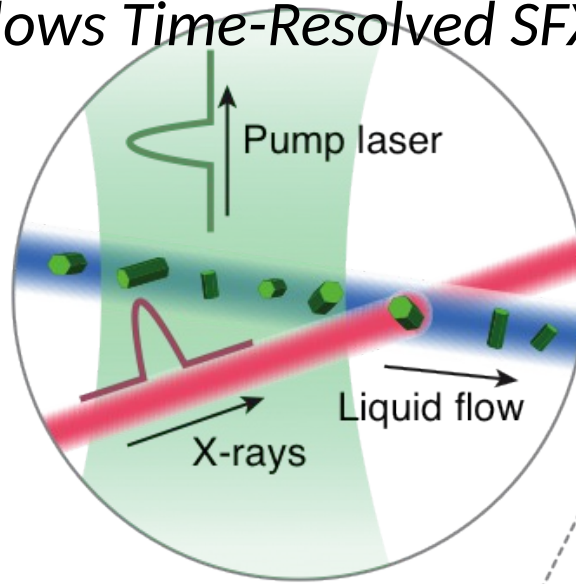
Pump laser off



Pump laser on

“Diffraction before destruction”
(next talks, Hadju, Chapman, Neutze)

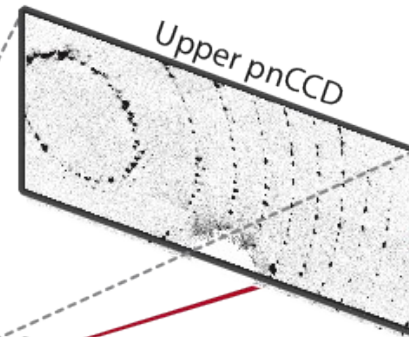
LCLS beam
2 keV X-ray energy
40 fs pulse duration



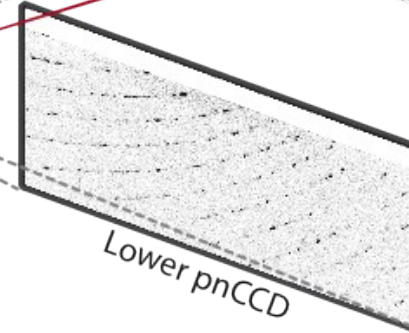
Gas dynamic
virtual nozzle

Optical fibre
laser coupling

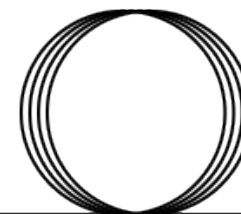
The 10 fs XFEL pulses should allow us to improve on the ~ 100 ps time resolution of SR (at RT, without damage).



Upper pnCCD



Lower pnCCD



Nd:YLF pump laser



Linear Coherent Light Source at SLAC > 2009

Weierstall, Doak and Spence, Rev Sci Instr. 2011.

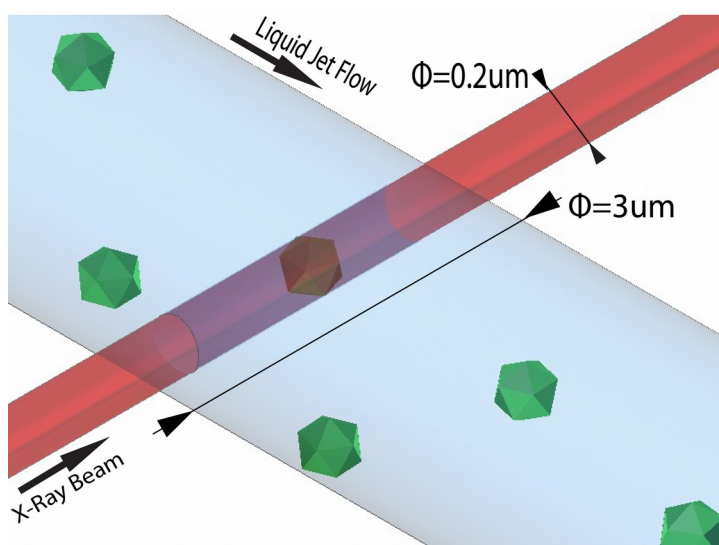
Why use an XFEL for structural biology ? (to image molecular machines at work)

- Avoid radiation damage. The smallest xtals fry before they'd give Bragg spots on synchrotron, reverse at XFEL.
- Room temp structures, avoid “freezing”.
- Better time resolution (ps).
- Irreversible reactions can be studied (eg PSI-ferredoxin).
- Xtals large enough for MX not available.
- Optical pump laser absorption length comparable to nanoxtal size.
- Diffusion times short for nanoxtal in mixing jet. Diffusive mixing possible.
- Higher resolution for some proteins. (Higher dose, 100X Safe Dose)
(Are smaller xtals or beam better ? **Dose, defects, diam of beam, DW.**
Depends on type of defect (SRO, LRO))

The STC supports four kinds of snap-shot diffraction experiments .

Note dimensions in microns.

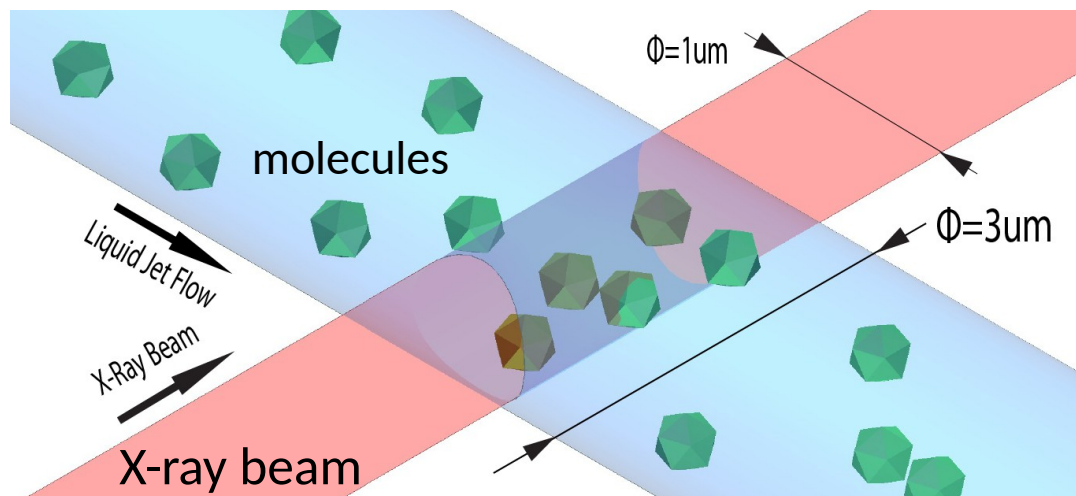
SFX, SP, FSS, 2D Xtals and TR variants.



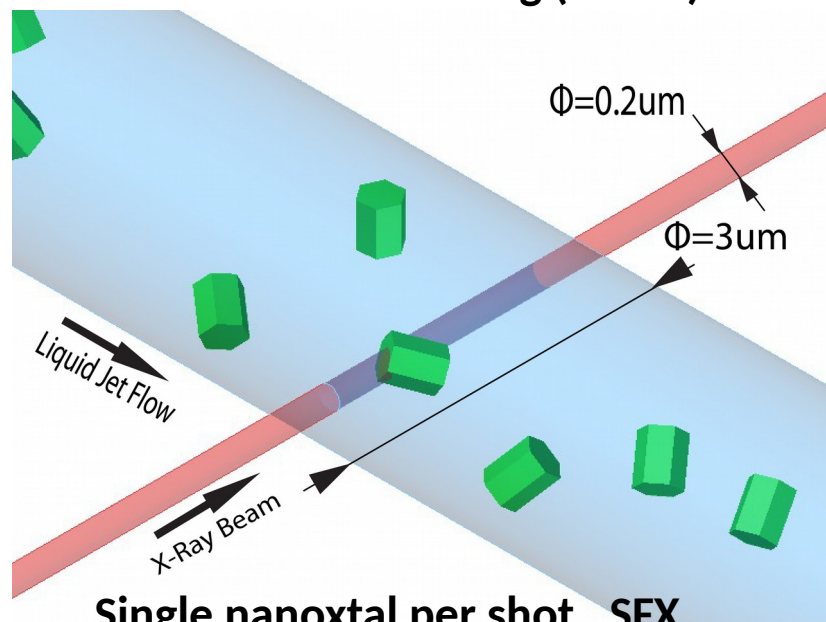
Single particle (eg virus) per shot . SP

Many X-ray shots do not hit a crystal

Plus 2D xtals on fixed targets (M. Frank)



Fast Solution Scattering (WAXS) FSS

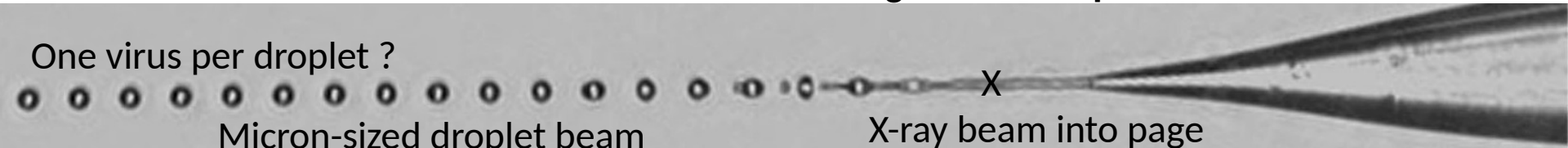


Single nanocrystal per shot. SFX

One virus per droplet ?

Micron-sized droplet beam

X-ray beam into page



Why is crystallography hard to beat ?

Current XFELs are not powerful enough to image single mols at high resolution

Bragg boost needed for atomic resolution, to see building blocks, how molecular machines work. Coherent amplification, so $I \sim n^2$ at one detector point, like 1D grating,

SASE Boost: XFEL also gives N^2 (for N electrons/bunch)

- *both N^2 needed to see atoms.*

Not possible using XFEL with SP (5 -12nm best in 2D, 3D worse) or FSS. ($I \sim \Theta^{-4}$). Modelling !

Crystallography is a filter for conformation.

Xtallog spreads the dose to avoid damage – less than damage dose per mol. XFEL solves this.

BUT the XFEL “stills” give wrong ratio of structure factors because of angular width of spots

And TR-SFX can only study limited protein motions which don't destroy the crystal.

Building blocks of matter are larger for biology than in condensed matter – secondary structure.

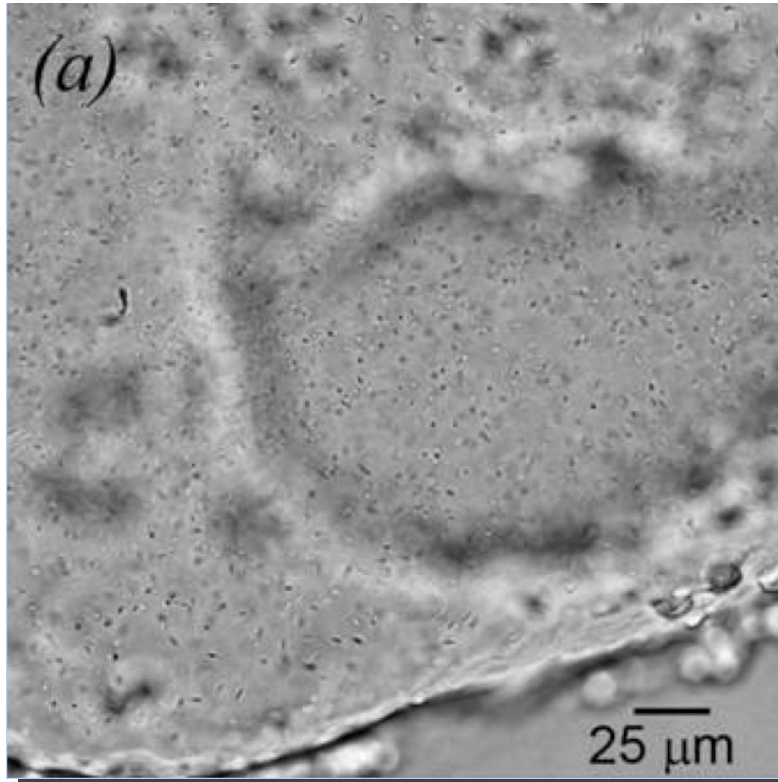
self-amplified *spontaneous* emission

The 14 high-resolution XFEL crystal structures published to March 2015.

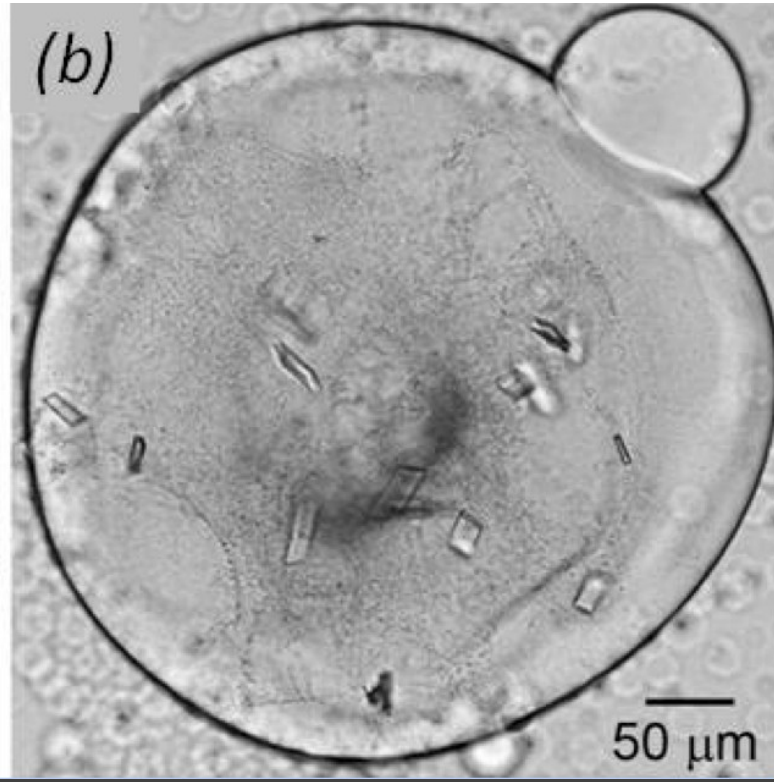
Date	Citation	Structure	Total Number of shots	Number of Indexed pattern used	Amount of protein	Comments
Jul-2012	Boutet	1.9 Å Lysozyme	66,442	12,247		
Jan-2013	Redecke	2.1 Å Cathepsin B	293,195	178,875		
Dec-2013	Liu	2.8 Å Serotonin receptor	152,651	32,819		
Jan-2014	Barends	2.1 Å Gadolinium lysozyme	191,060	59,667		
Feb-2014	Weierstall	3.2 Å Smoothens GPCR	152,651	32,819	0.5 mg	
May-2014	Hattne	2.1 Å Thermolysin	14,932	11,455		
Sep-2014	Sawaya	2.8 Å Cry3A Toxin	380,650	78,642		
Dec-2014	Tenboer	1.6 Å Photoactive Yellow Protein	36,632	22,678	300 mg	CASPAD hi/low gain
Dec-2014	Cohen	1.6 Å Hydrogenase	162	158		Postrefinement
Dec-2014	Cohen	1.36 Å Myoglobin	932	739		Goniometer, Mar
Mar-2015	Ginn	1.75 Å CPV17 Polyhedrin	144,803	5,787		Postrefinement
Forthcoming	Xu	3 Å GPCR-arrestin complex	8934	2047		

Vadim Cherezov

- These span the cell membrane. About human 800 GPCRs respond to many extracellular signaling molecules and transmit signals into the cell
- 40% of drugs target GPCRs. 70% of recent drug approvals were GPCRs
- Challenges: low expression yields, low receptor stability after extraction from native membranes with detergent, high conformational heterogeneity
- 19 receptor structures solved so far
- most were crystallized in LCP
- crystals often limited in size, sub 10 micron
- microfocus beamlines have been used, radiation damage severe, merge data from multiple crystals.



A typical initial hit contains high-density of $3 \times 1 \times 1 \mu\text{m}^3$ crystals suitable for XFEL.

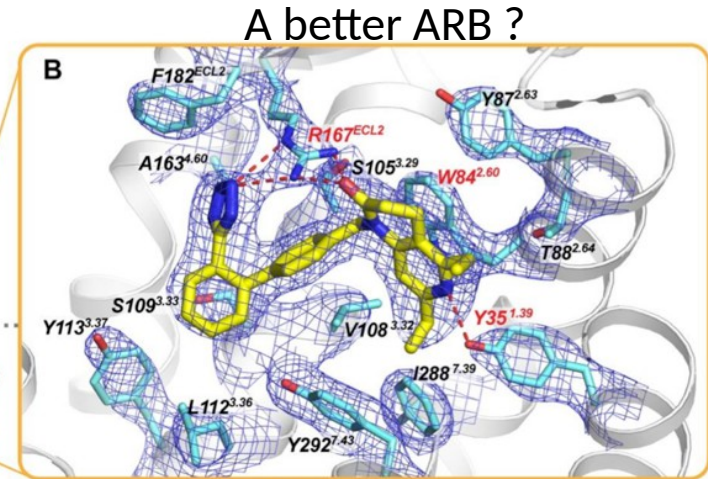
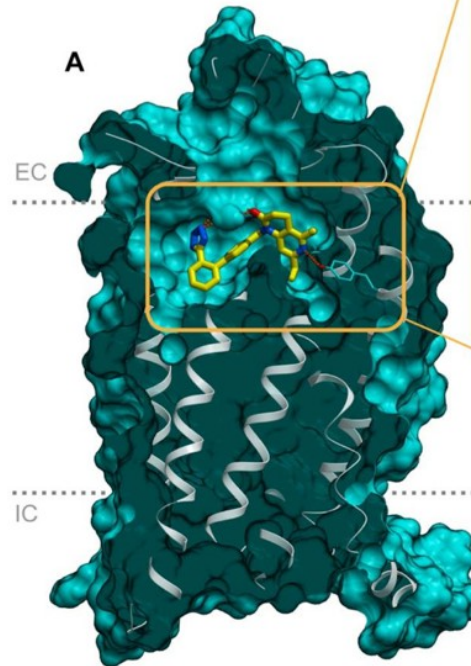


Substantially larger crystals ($40 \times 20 \times 7 \mu\text{m}^3$), required for microfocus synchrotron data collection, were produced after one year of intensive optimization studies.

Vadim Cherezov

- Serves as a primary regulator for blood pressure maintenance
- In complex with a selective antagonist ZD7155
- We got 2.9 Å resolution (vs 4 Ang with SR, twinned)

GOAL 1. Develop SFX.



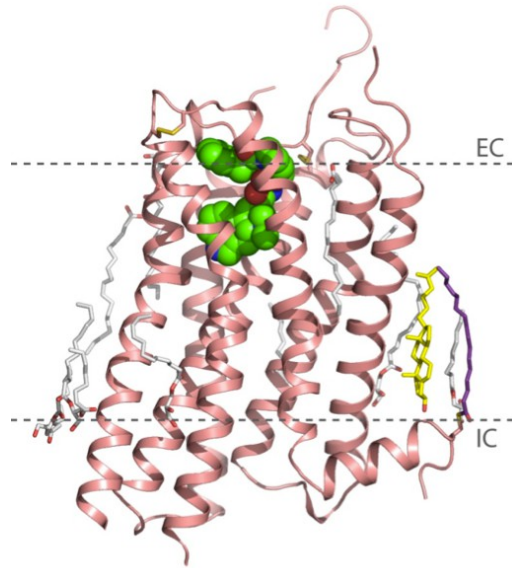
AT1R - ZD7155 (yellow) complex

Despite its medical importance, structure is unknown, due to limited crystal size.

***First novel GPCR structure solved with SFX**
***Better res than SR.**

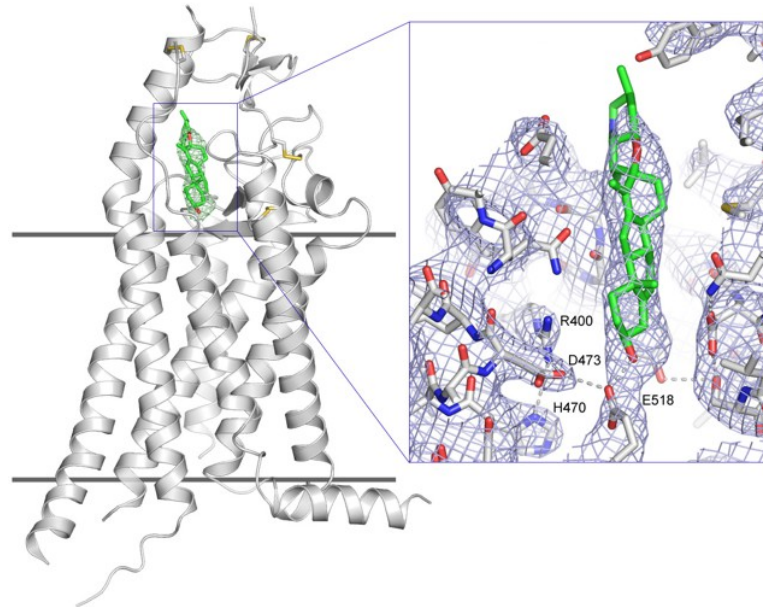
Fusion proteins added assist crystallization. Serotonin, δ -opioid, plus 4 other GPCRs....

Additional SFX results from microcrystals in LCP



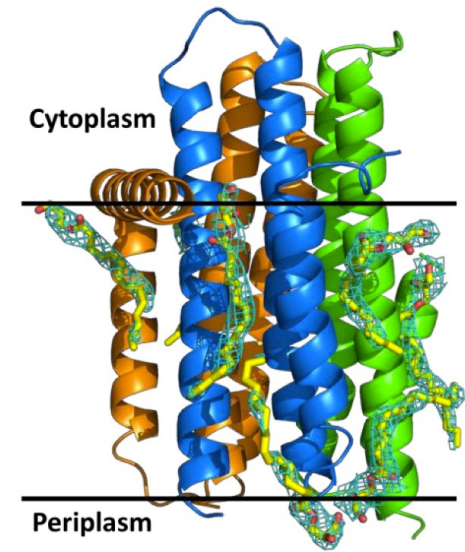
Serotonin receptor with
ligand ergotamine
(2.8 Å)
indexed patterns: 32,819

Wei Liu...Science 20, 2013:
342 1521-1524



Smoothed receptor with
ligand cyclopamine
(3.8 Å)
indexed patterns: 40,036

Weierstall...Nature Communications
5: 3309, 2013



Membrane Kinase DgKA
(2.8 Å, March 2013)
indexed patterns: 66,165
unpublished

Also: δ -Opiate receptor* (+ DIPP-NH₂), and human rhodopsin bound to arrestin (Xu et al)

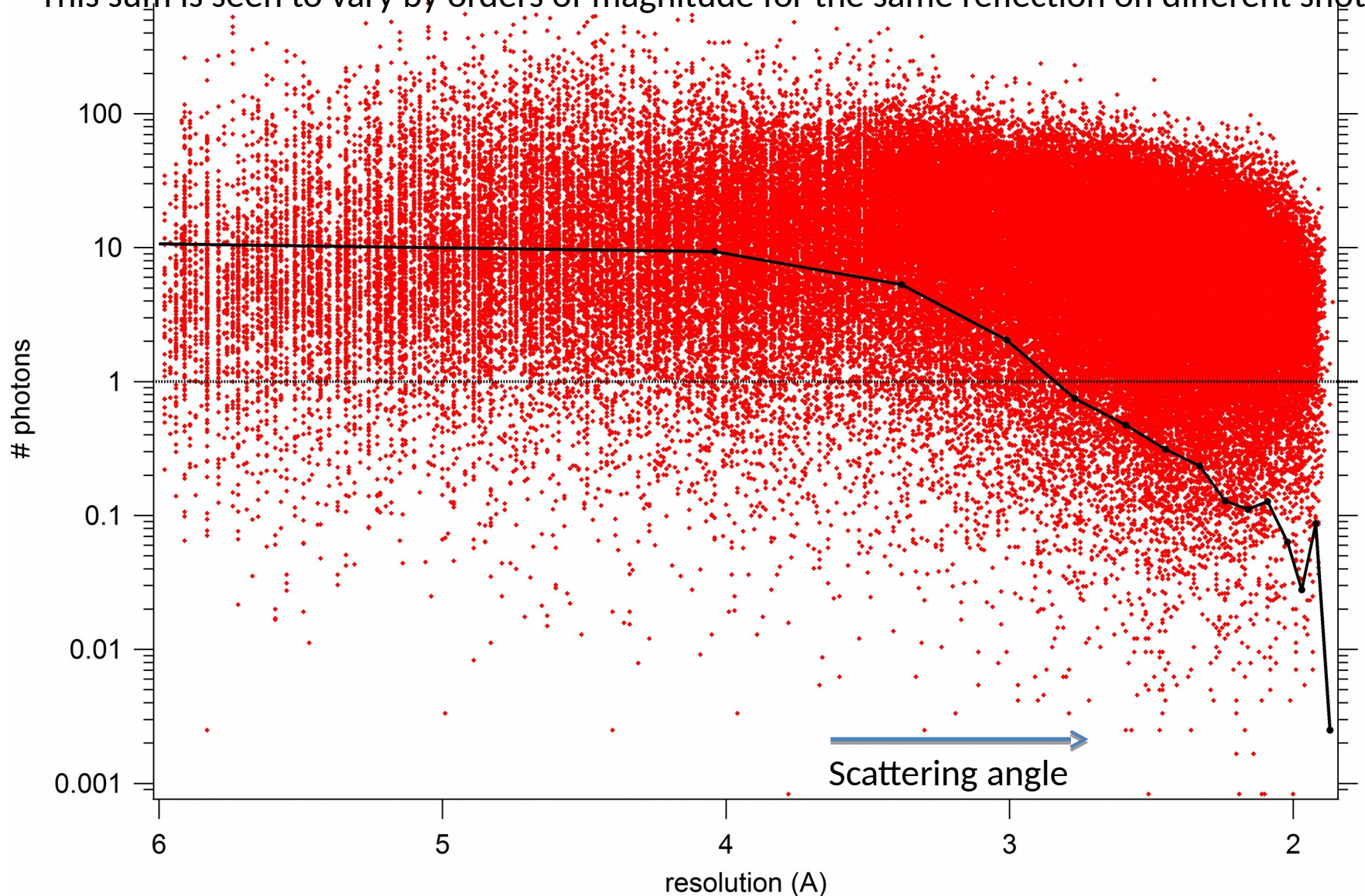
0.3 mg protein for full data set, compare to sample consumption with
GDVN injector: 10 - 15 mg of protein. *reduce pain-killer addiction

Vadim Cherezov,
Martin Caffrey

Data Analysis

What the nanoxtal Bragg XFEL data looks like

SFX Each point is the sum of all pixels contributing to one partial reflection on one shot. This sum is seen to vary by orders of magnitude for the same reflection on different shots.



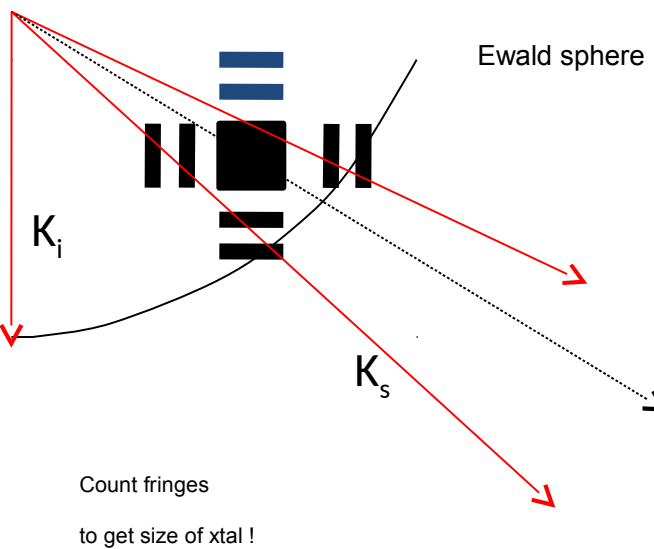
Granulo Virus nanoxtal data. Tom White. Negative intensities shift mean. Nov 2014.

New data merging algorithms take account of partial reflections.

Snapshot diffraction has no goniometer ! Rossman's "American Method".

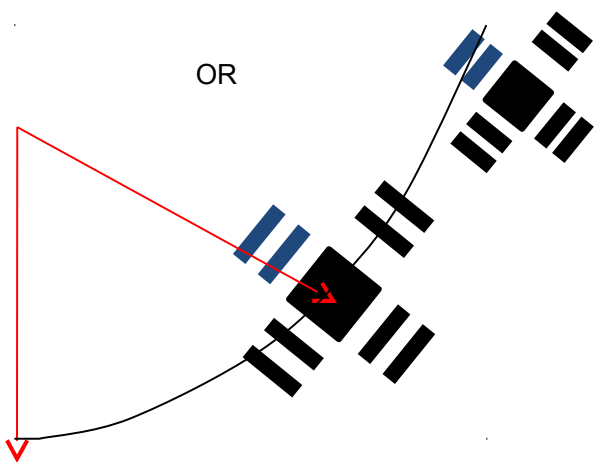
In XRD the Ewald sphere takes a SLICE through the 3D FT of the nanocrystal shape

But the structure factors are proportional to the VOLUME of the shape-transform.

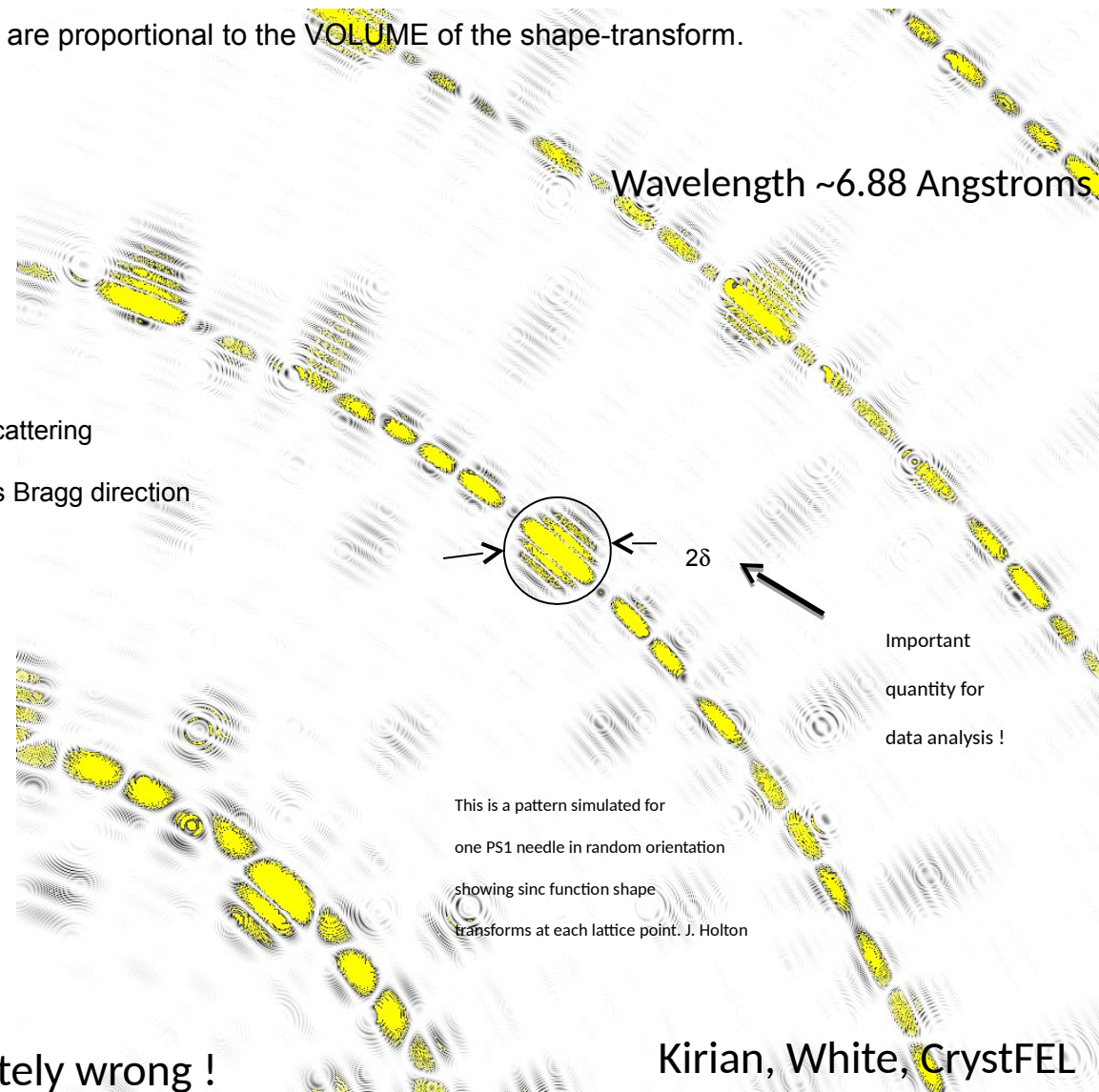


No scattering
in this Bragg direction

OR



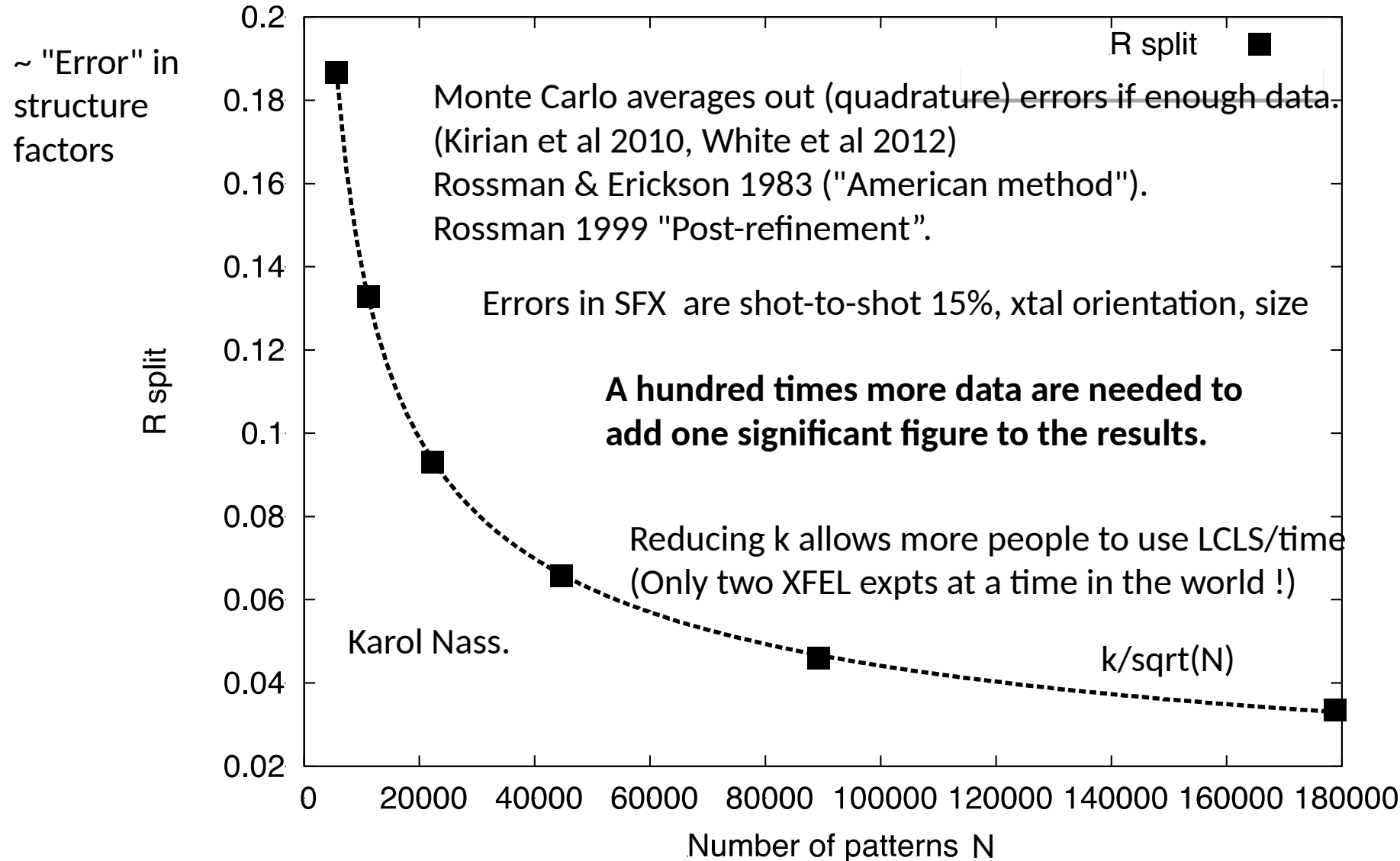
Ratio of Bragg intensities completely wrong !

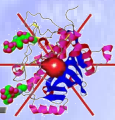


Kirian, White, CrystFEL

The Monte Carlo method for SFX reduces error as k/\sqrt{N}

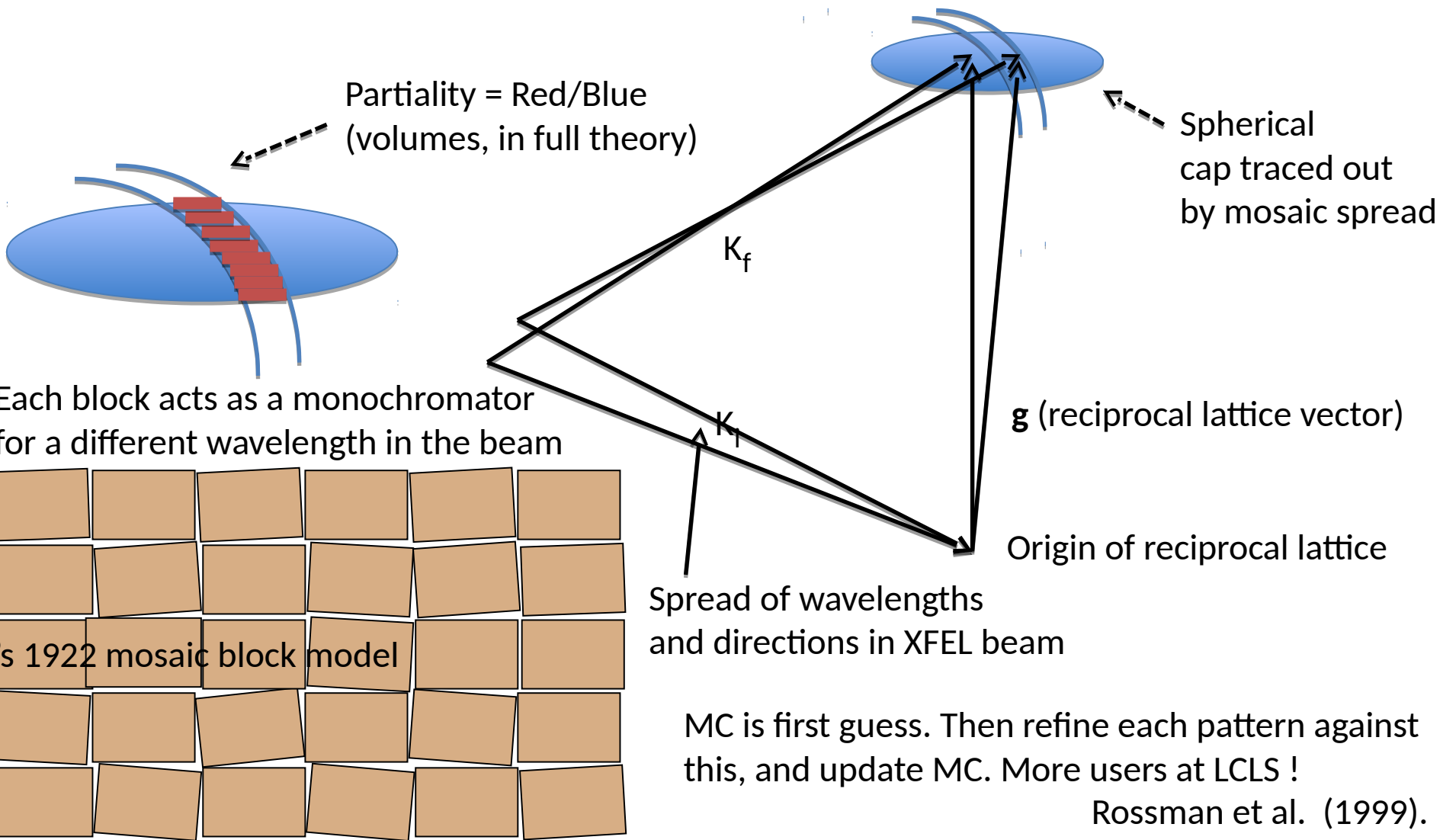
Data for Cathepsin, LCLS

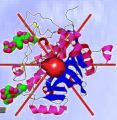




New algorithms in Year 2 take account of partiality and mosaic spread

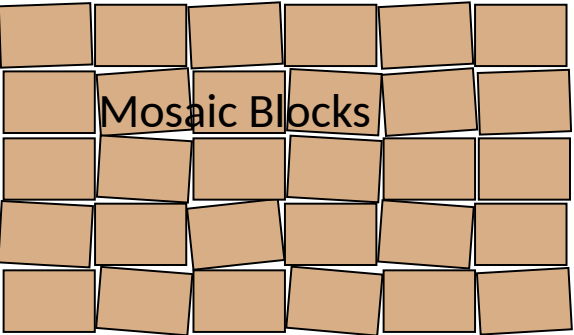
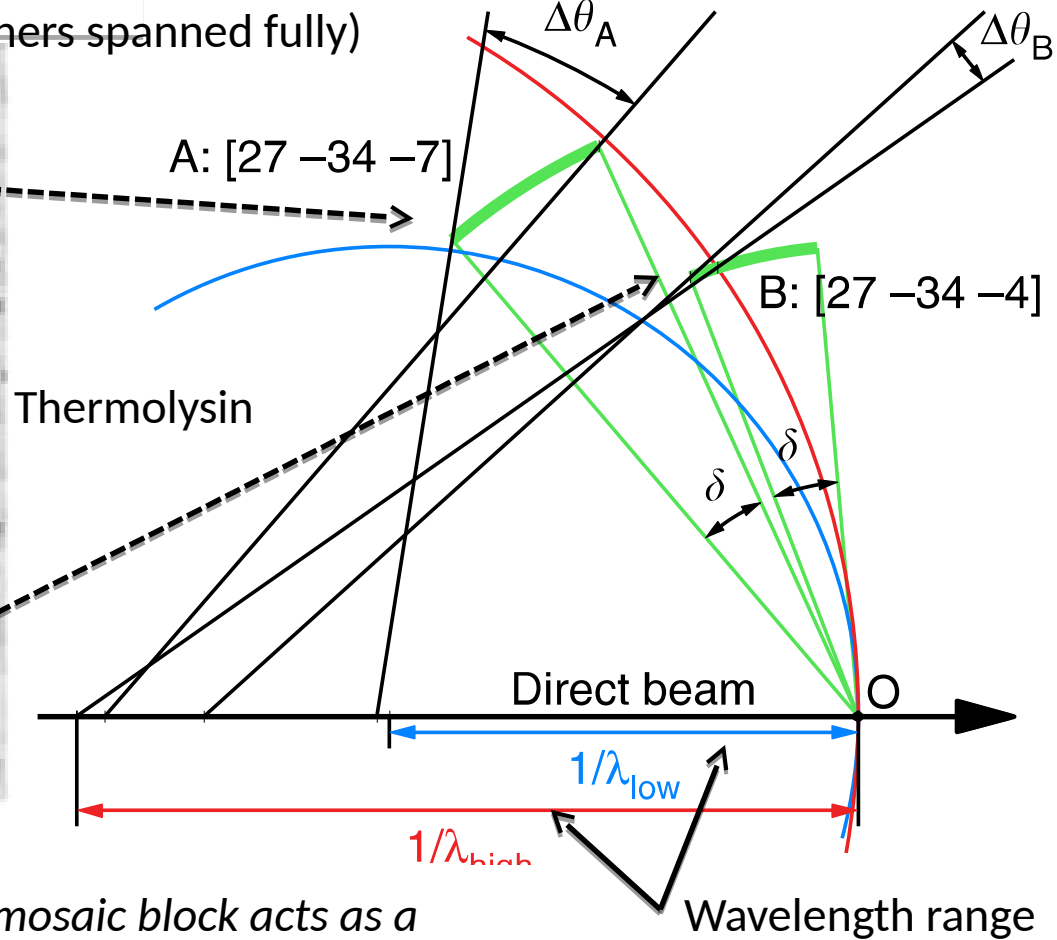
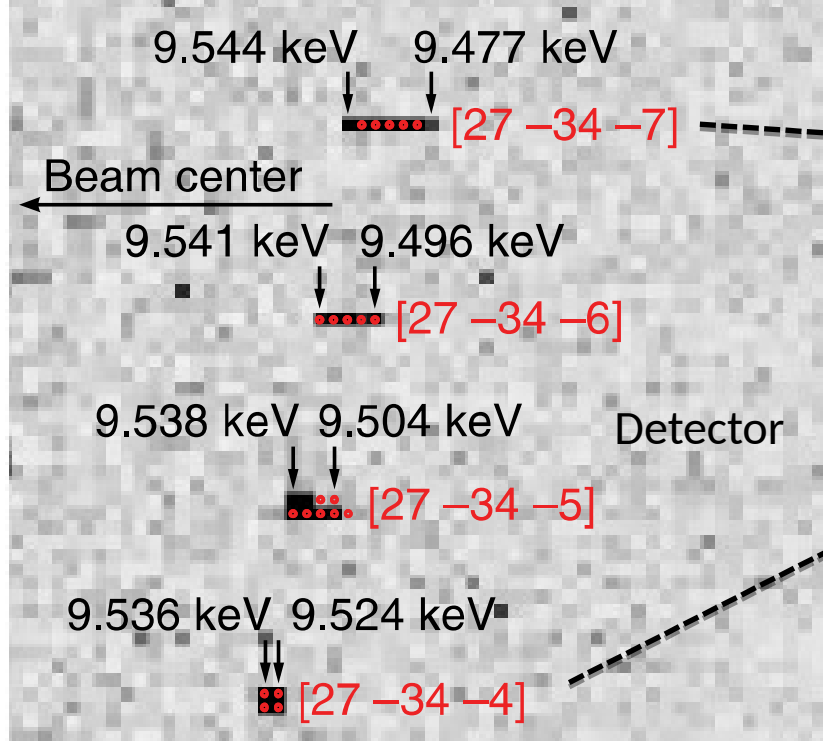
SFX data sets now small enough to allow iterative optimization of experimental params (λ , S_g) on every shot – beyond Monte Carlo (MC) averaging. (White, Ginn, Sauter, Brunger, Kapsch...)





The wavelength spread in XFEL beam spans wider spots at higher angle.

so different fractions of different reflections are uncovered by the range of wavelengths.
 (some reflection blobs are just clipped, others spanned fully)



Each tilted mosaic block acts as a monochromator for a different component wavelength in the beam..

Developments in sample delivery

The coefficient A is to be determined from the consideration that the outwards normal velocity at the surface of the cylinder is equal to $\dot{a} \cos \alpha z$. Hence

$$icA J_0'(ica) = \dot{a} \dots \dots \dots (10).$$

Denoting the density by ρ , we have for the kinetic energy the expression

$$T = \frac{1}{2} \rho \int 2\pi a \cdot \phi \frac{d\phi}{dr_{(z=a)}} dz;$$

or, if we reckon it in the same way as V per unit of length,

$$T = \frac{1}{2} \rho \pi a^2 \frac{J_0(ica) \dot{a}^2}{ica J_0'(ica)} \dots \dots \dots (11).$$

Thus, by Lagrange's method, if $a \propto e^{qt}$,

$$q^2 = \frac{T_1}{\rho a^3} \frac{(1 - \kappa^2 a^2) \cdot ica \cdot J_0'(ica)}{J_0(ica)} \dots \dots \dots (12),$$

which determines the law of falling away from equilibrium for a disturbance of wave-length λ . The solutions for the various values of λ and the corresponding energies are independent of one another; and thus, by Fourier's theorem, it is possible to express the condition of the system at time t , after the communication of any infinitely small disturbances symmetrical about the axis. But what we are most concerned with at present is the value of q^2 as a function of κa , and especially the determination of that value of κa for which q^2 is a maximum. That such a maximum must exist is evident *a priori*. Writing x for κa , we have to examine the values of

$$\frac{(1-x^2) \cdot ix \cdot J_0'(ix)}{J_0(ix)} \dots \dots \dots (13).$$

Expanding in powers of x , we may write, for (13),

$$\frac{1}{2} x^2 (1-x^2) \left\{ 1 - \frac{x^2}{2^2 \cdot 3} + \frac{x^4}{2^4 \cdot 3} - \frac{11x^6}{2^6 \cdot 3} + \frac{19x^8}{2^8 \cdot 3 \cdot 5} + \dots \right\} \dots \dots (14).$$

or $\frac{1}{2} \left\{ x^2 - \frac{1}{2} x^4 + \frac{7}{2^4 \cdot 3} x^6 - \frac{25}{2^6 \cdot 3} x^8 + \frac{91}{2^8 \cdot 3 \cdot 5} x^{10} + \dots \right\} \dots \dots (15).$

Hence, to find the maximum, we obtain by differentiation

$$1 - \frac{1}{2} x^2 + \frac{7}{2^4 \cdot 3} x^4 - \frac{100}{2^6 \cdot 3} x^6 + \frac{91}{2^8 \cdot 3} x^8 + \dots = 0 \dots \dots \dots (16).$$

If the last two terms be neglected, the quadratic gives $x^2 = .4914$. If this value be substituted in the small terms, the equation becomes

$$.98928 - \frac{1}{2} x^2 + \frac{7}{16} x^4 = 0,$$

whence $x^2 = .4858 \dots \dots \dots (17).$

The corresponding value of λ is given by

$$\lambda = 4.508 \times 2a \dots \dots \dots (18),$$

which gives accordingly the ratio of wave-length to diameter for the kind of disturbance which leads most rapidly to the disintegration of the cylindrical mass. The corresponding number obtained by Plateau from some experiments by Savart is 4.38, but this estimate involves a knowledge of the coefficient of contraction of a jet escaping through a small hole in a thin plate, and is probably liable to a greater error than its deviation from 4.51.

The following table exhibits the relationship between x^2 or $\kappa^2 a^2$ and the square root of expression (13) to which q is proportional:—

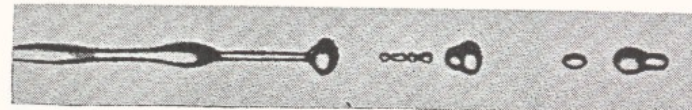


Fig. 5.15

Rayleigh's experiments with tuning fork and spark-gap flash photography 1878

Necking instability has period = 4.5 D.
(consider KE and Surf En of liquid column)

Rate of droplet formation given by buzzer.

* Phil. Mag., Vol. xxxvi. 1868. † Phil. Mag., Nov. 1871.

TR Protein nanoxtal sample delivery uses a liquid jet

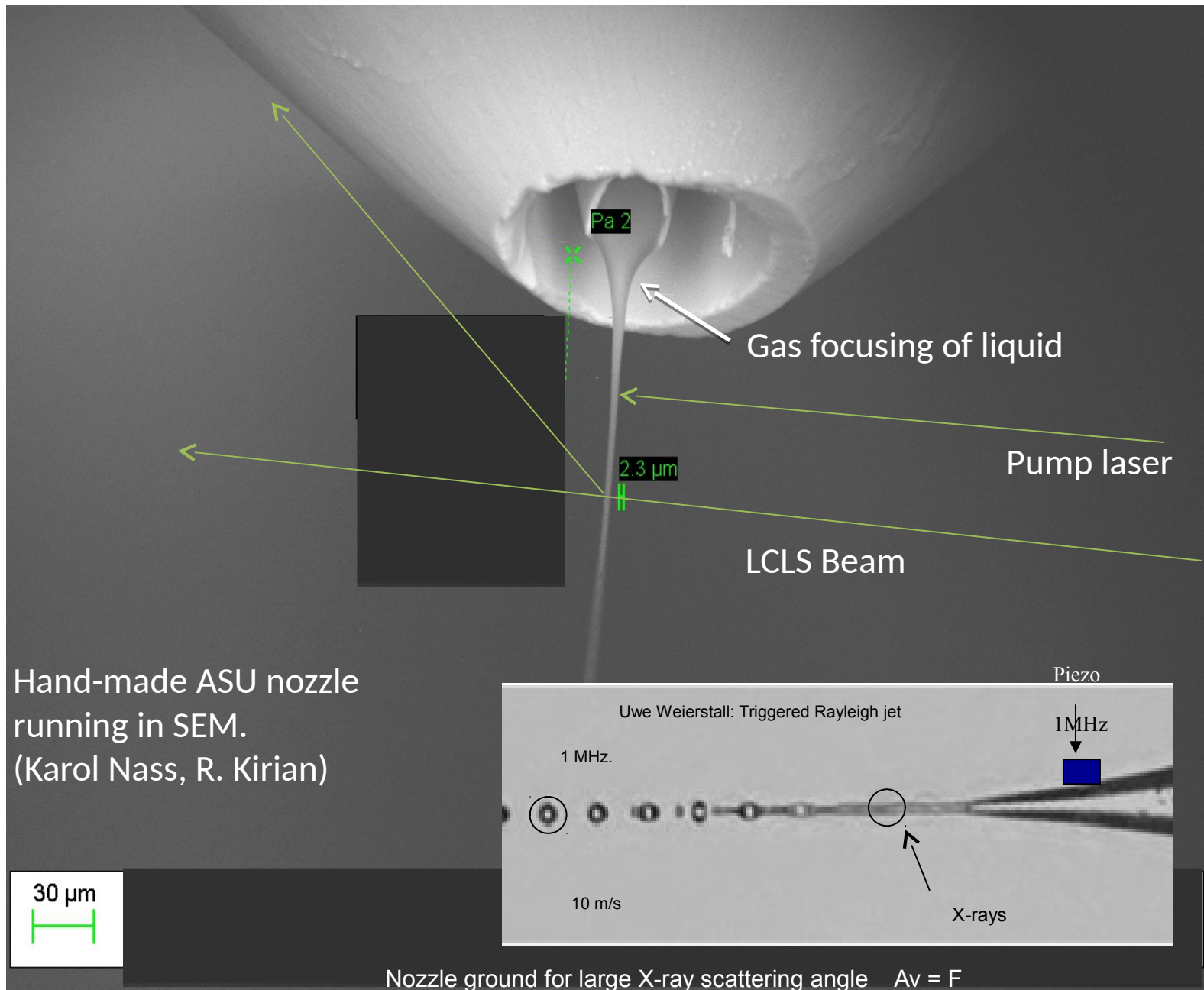
Droplets freeze
at 10^6 /sec.

in vacuum
to vitreous
ice if cryo
protectant used

Flow velocity
about 10 m/sec

Area * velocity
= flow rate
= constant.

Hand-made ASU nozzle
running in SEM.
(Karol Nass, R. Kirian)



Nozzle ground for large X-ray scattering angle $Av = F$

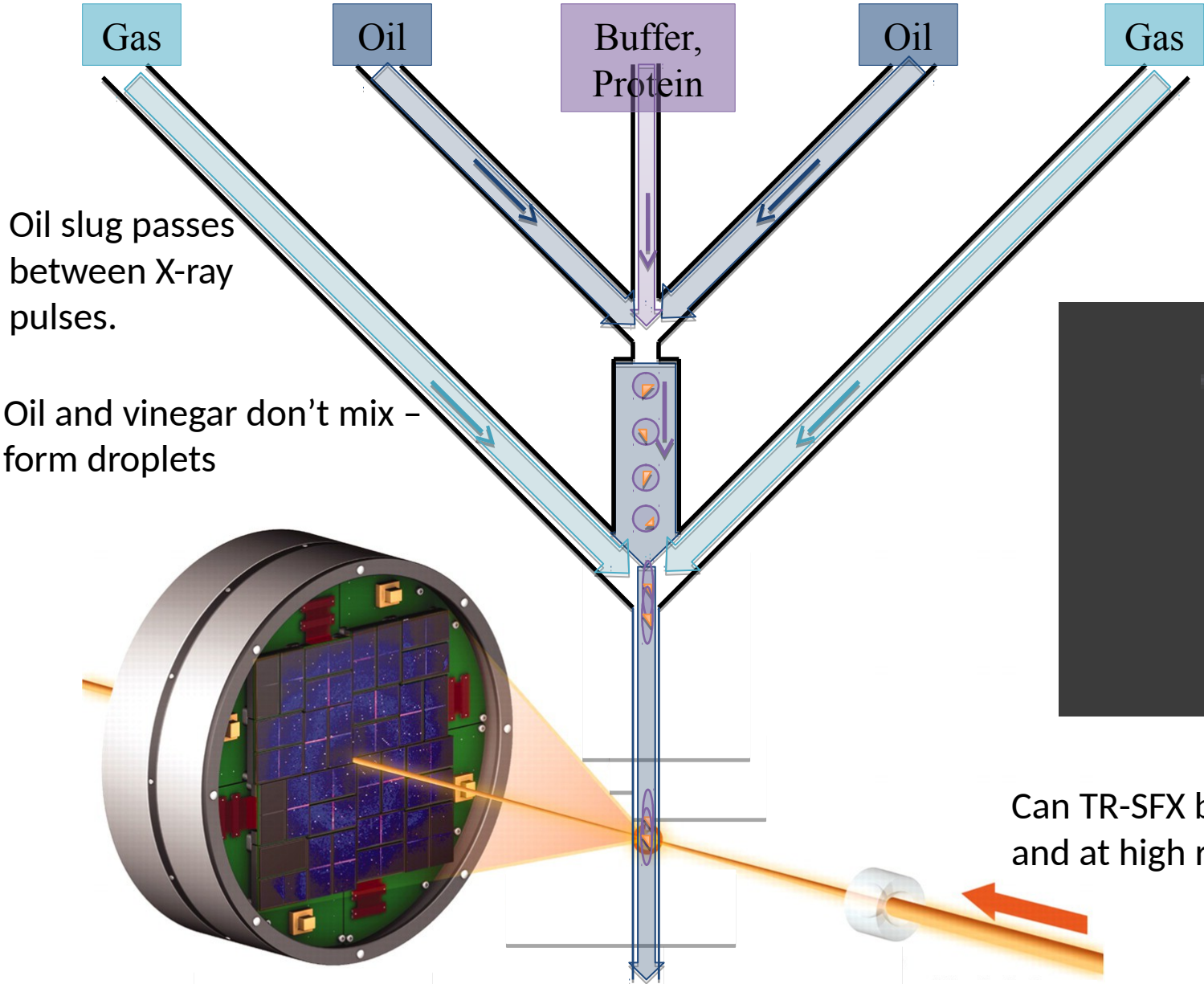
Sample waste in liquid jet currently

movie



This waste can be greatly reduced by switching off the jet between X-ray pulses.

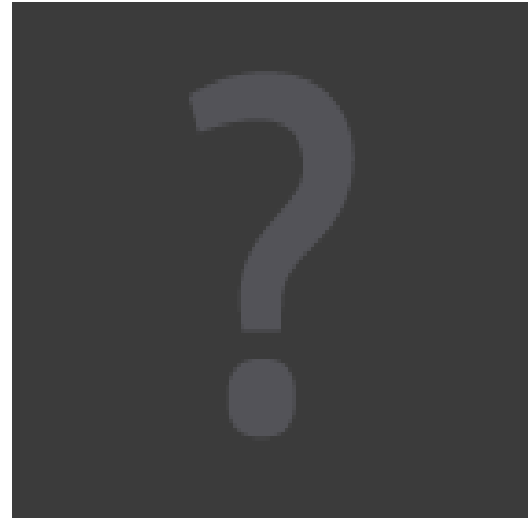
We are developing a switching jet to reduce sample volume for liquid jet (TR-SFX)



The ASU Switching GDVN jet alternates oil and protein slugs across X-ray beam

Oil slug passes between X-ray pulses.

Oil and vinegar don't mix - form droplets



Can TR-SFX be done with this and at high rep-rate for LCLS 2 ?

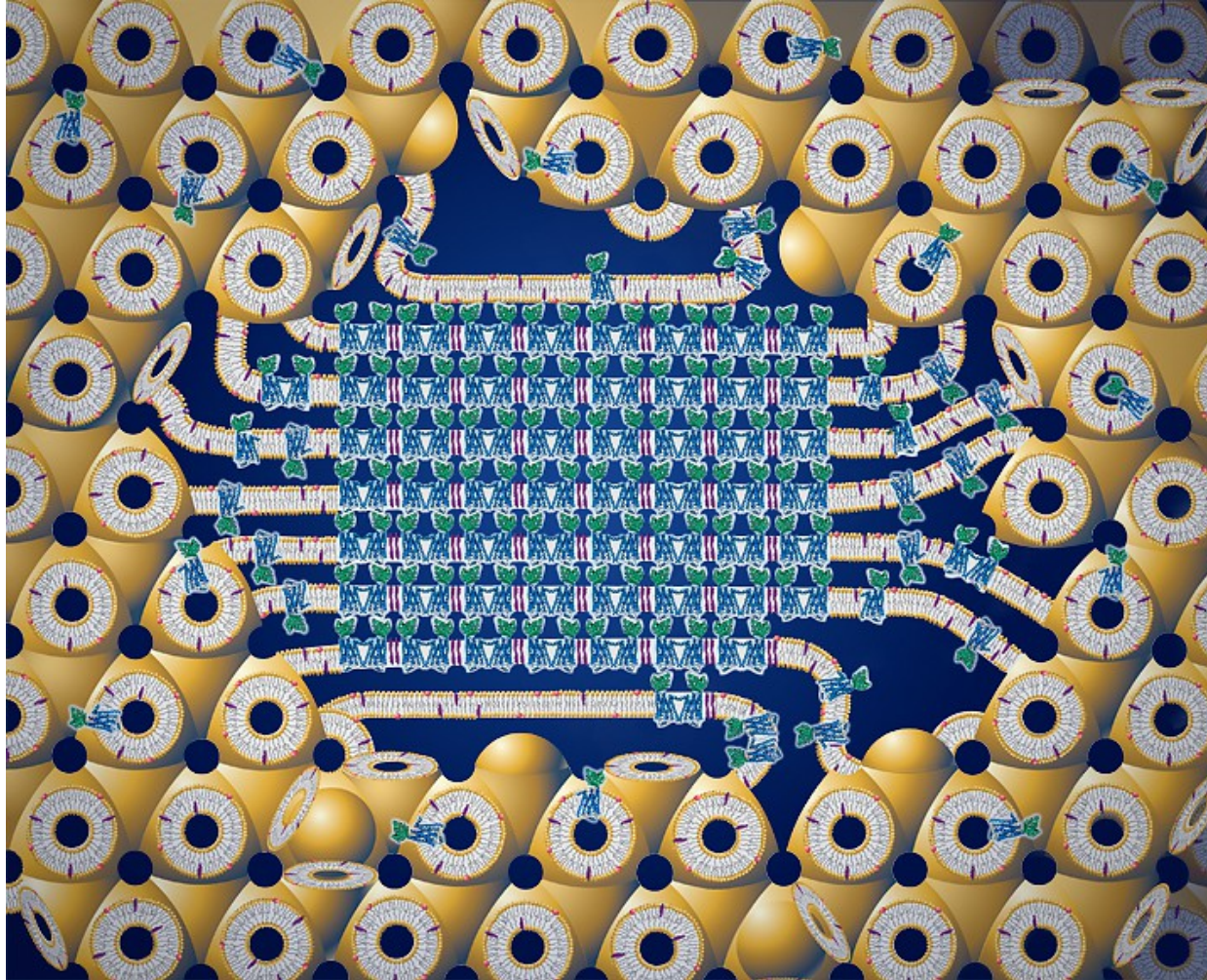
Some membrane protein nanocrystals (& others) grow in Lipid Cubic Phase

Membrane protein embedded within lipid cubic phase (viscosity of car grease !)

Works for soluble proteins too..

0.1 mg of Lys. used rather than 15 mg in Boutet (2012) with GDVN OR 6,000 xtas of phycocyanin to 1.95 Å.

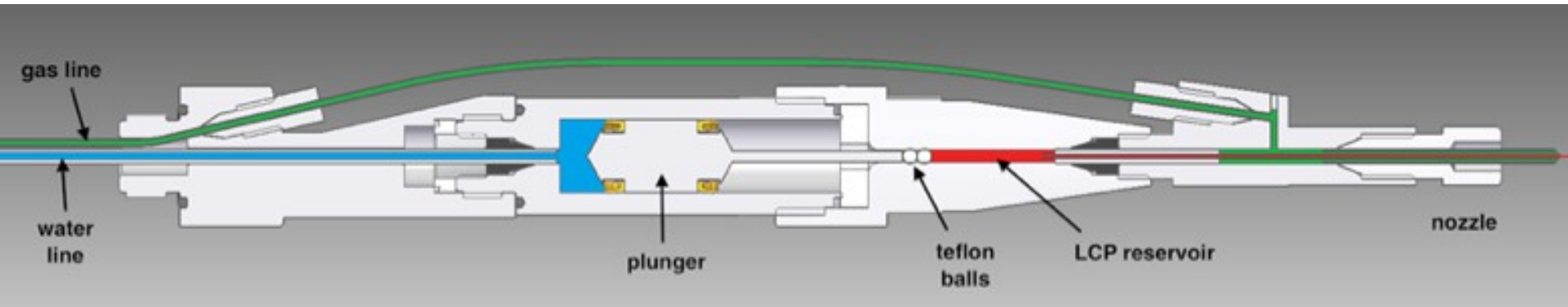
Cherezov Talk !!



Martin Caffrey

Water jet flows at 10/s (10 microns/microsec). Can higher viscosity match nanocrystal flow rate to arrival of X-ray pulses at 100 Hz ? TOOTHPASTE JET !!!!

A grease gun to deliver nanocrystals to the XFEL in LCP.



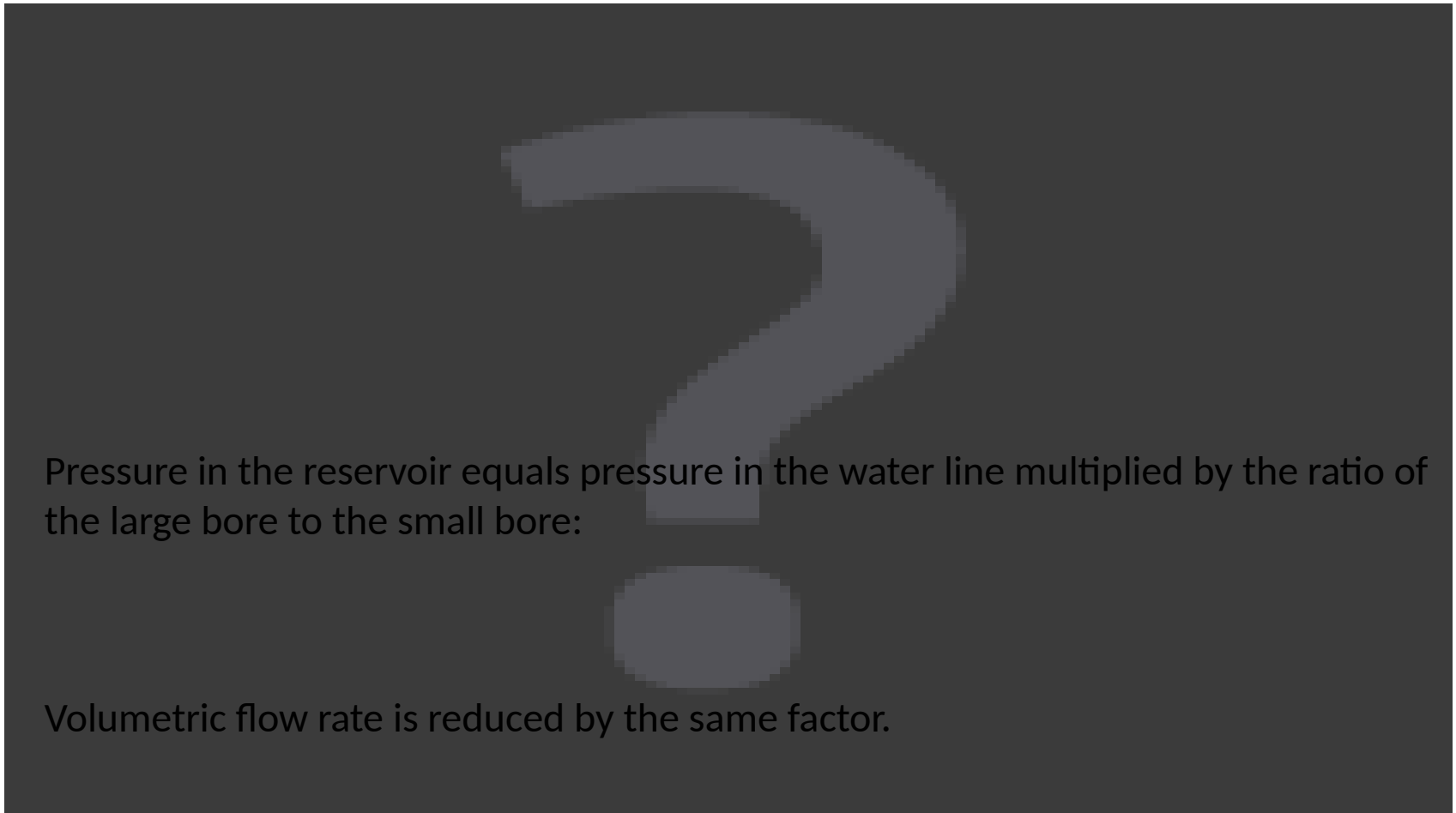
- * LCP provides a **growth** medium for many proteins, including membrane proteins.
- * LCP jet delivers ptcls at about the **rate** of X-ray pulses.
- * Low flow rate avoids **wasted** protein (1-300 nl/min vs 10 microL/min in water jet).
- * Use less protein of precious human protein, eg 0.3 milligrams

**Used to solve Cyclopamine GPCR binding to smoothen receptor (3 A)
Angiotensin, δ -OR, Serotonin.**

**New media support PSI, PSII, Phycocyanine, Cytochrome C oxidase,
Rhodopsin, Sindbis nanocrystals.**

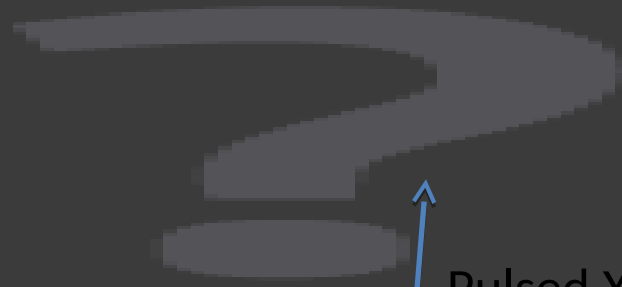
The asymmetric piston provides an amplification in pressure.

Movie



“Toothpaste” jet

LCP jet operating at LCLS



Pulsed X-ray beam

50 μm

Optimize conc, rep rate,
viscosity, chemistry, particle
size, jet size, for each sample.
 $V = F/A$ $AV = \text{const.}$

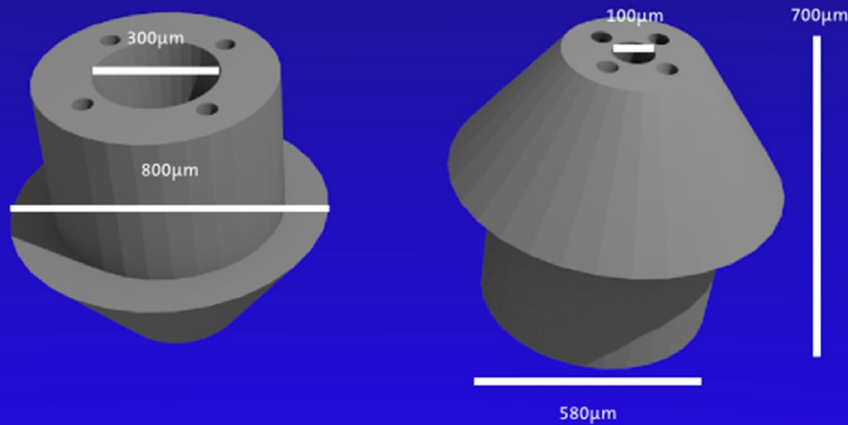
XFEL beam drills 120 holes/sec across LCP tube.
Adjust flow speed to avoid shrapnel from last hole
Gaps due to time-structure of LCLS pulses.

Agarose also works for soluble proteins.
Conrad et al IUCrJ in press. Phycocyanine to 2.6 Ang.

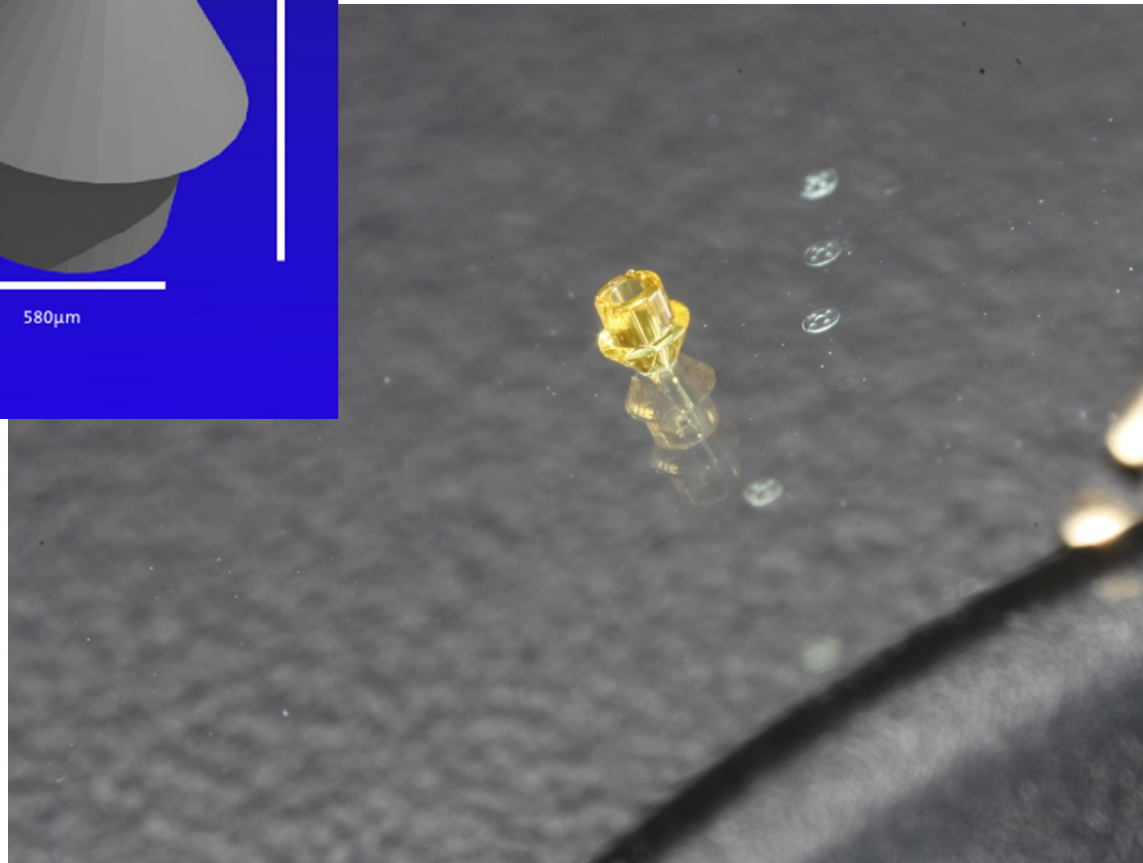
GPCR in viscous LCP at 300 picoliters per minute. LCLS at 1 Hz. 9.4 kV 7% attenuation
50 microliters total used Later 5 microliters/min.

Also works at synchrotrons ! MSX 2 Ang Resolution in bR @ ESRF – Standfuss, Schertler.

CAD design and result after printing



STC Collaboration with Nanoscribe, Germany.



Top: Dimension of the nozzle

Two-photon polymerization is a direct-write process with 100nm resolution.

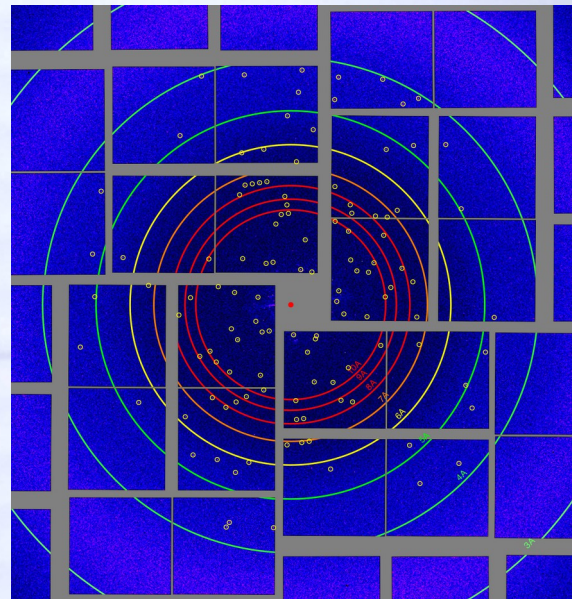
Right: 3D printed nozzle on substrate

First result of 3D printed GDVN nozzle, made to ASU design at Nanoscribe, Germany

Enables flexible prototyping, optimization from CAD of mixing, switching, sheet jets etc.

Proposals for 3D printer sent to : NIH High-end Instrumentation; NIH Shared Instrumentation ; NSF MRI ; Continue till funded.

Cost: \$500K



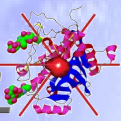
Cytochrome C Oxidase D. Rousseau
Extends to 4 Ang SFX LCLS

FIRST 3D (2PP) PRINTED NOZZLE RUNNING FEB 2015

Garret Nelson

Fabrication time 4 hours. Cost ~ \$1000. 2PP Printer cost \$500K (Handmade take 4 hours, "free")

- Integrated with microfluidics (Ros Lab) - nanoxtal size sorter using electrophoretics..



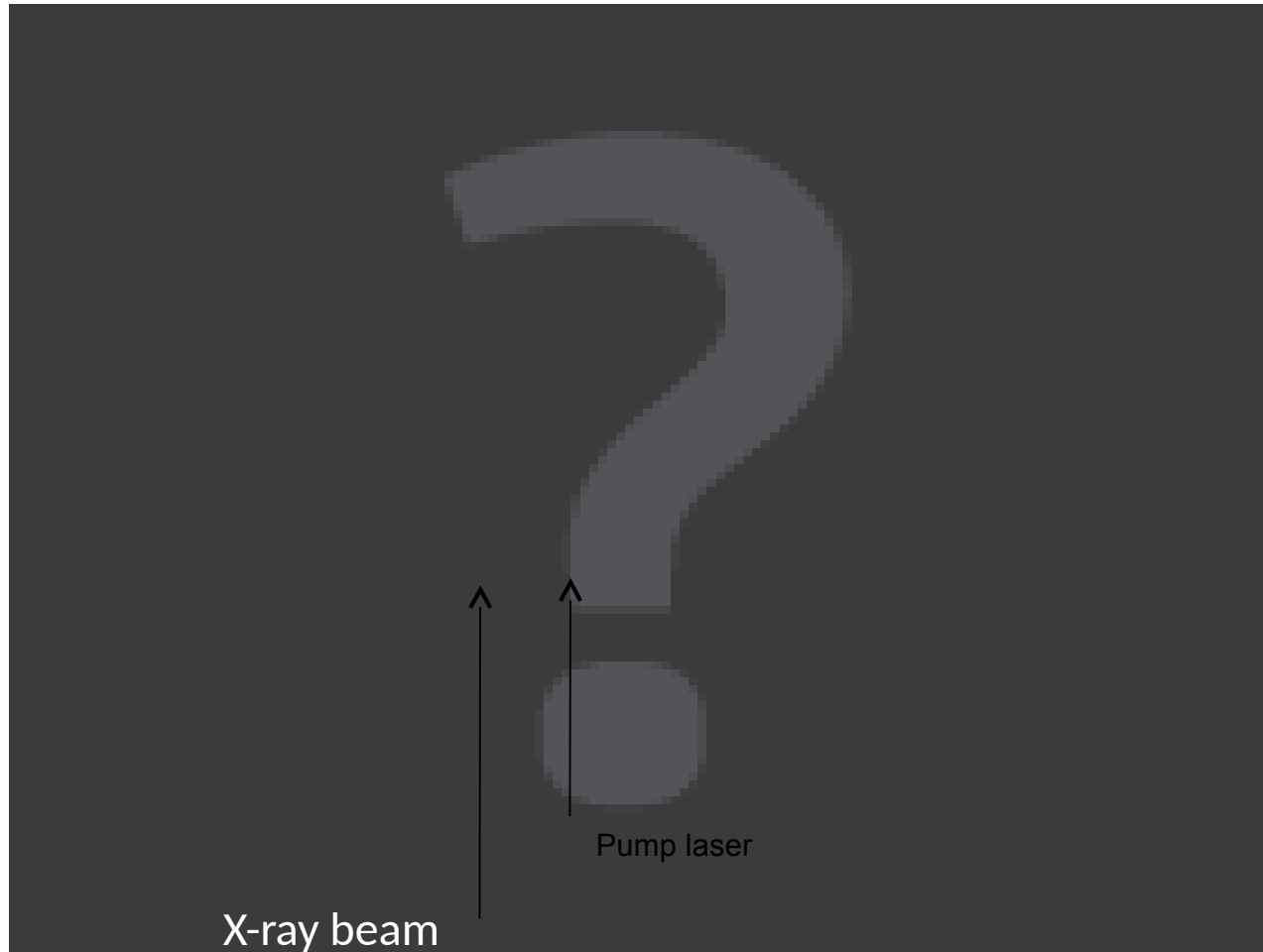
Development of Time-Resolved SFX

For *irreversible processes* – eg catalysis, enzymes

Pump-probe experiments are possible with the liquid jet.

Pump laser and XFEL on jet – exploding PS I nanocrystals

Like sunlight on a leaf....snapshots of the excited state density



pump
laser:532nm,
10ns pulse, 8
microjoules,
focused to 380
micron spot,
fiber coupled,

Time delay
between 70 fs
X-ray pulse
and laser 0 -
10 μ s

7 micron beam
0.5-2 mic. xtals
4 micron jet

To observe *undocking of ferredoxin from PSI*, excite xtal 10 microseconds before XRD snapshot

Travelling at 10 m/s, nanocrystals go 100 microns, less than width of 400nm doubled femtosecond beam

Movie

Aquila
Optics
Express
2012

Kupitz,
Fromme
et al
Nature
2014

TR-SFX of Photoactive Yellow Protein (now 1.4 Ang resolution). Blue light photoreceptor mechanism at 1 μsec & 10 ns time delays.

A light-sensor in purple **photosynthetic** bacteria

Pump light saturates nanoxal

Science Dec 2014

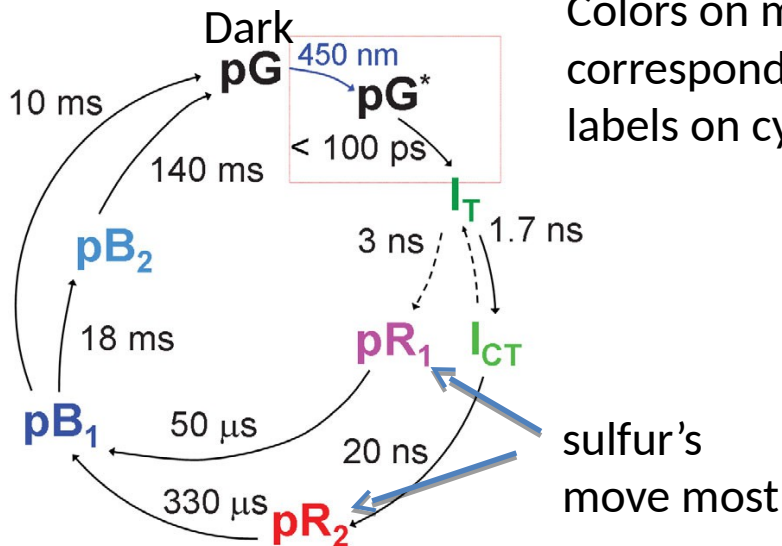
Tenboer... Marius Schmidt et al
group (Milwaukee) +STC

Delays 10ns and
1 microsec.

pR1 and pR2 are maximally
occupied at 1 microsec.

Red is PR1
then later
PR2. Not a
diff. map.

Colors on map
correspond to
labels on cycle



reaction rate lifetimes, exp decay. SVD
Six stable intermediates



Photoactive Yellow Protein, pR₁, pR₂, imaged at LCLS
Shows total density of intermediates that accumulate
and decay during the photocycle. Chromophores.

Time dependence of concentration of intermediate states

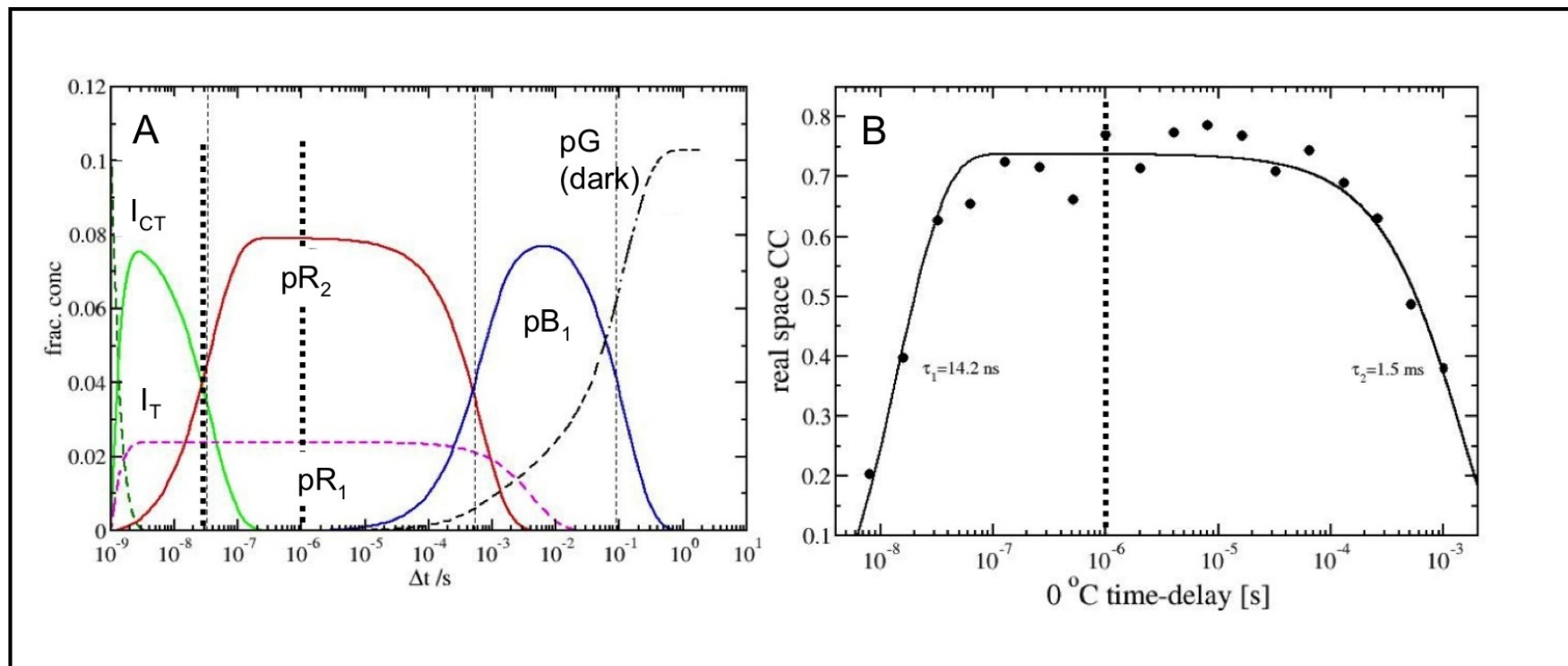
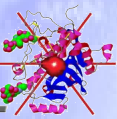


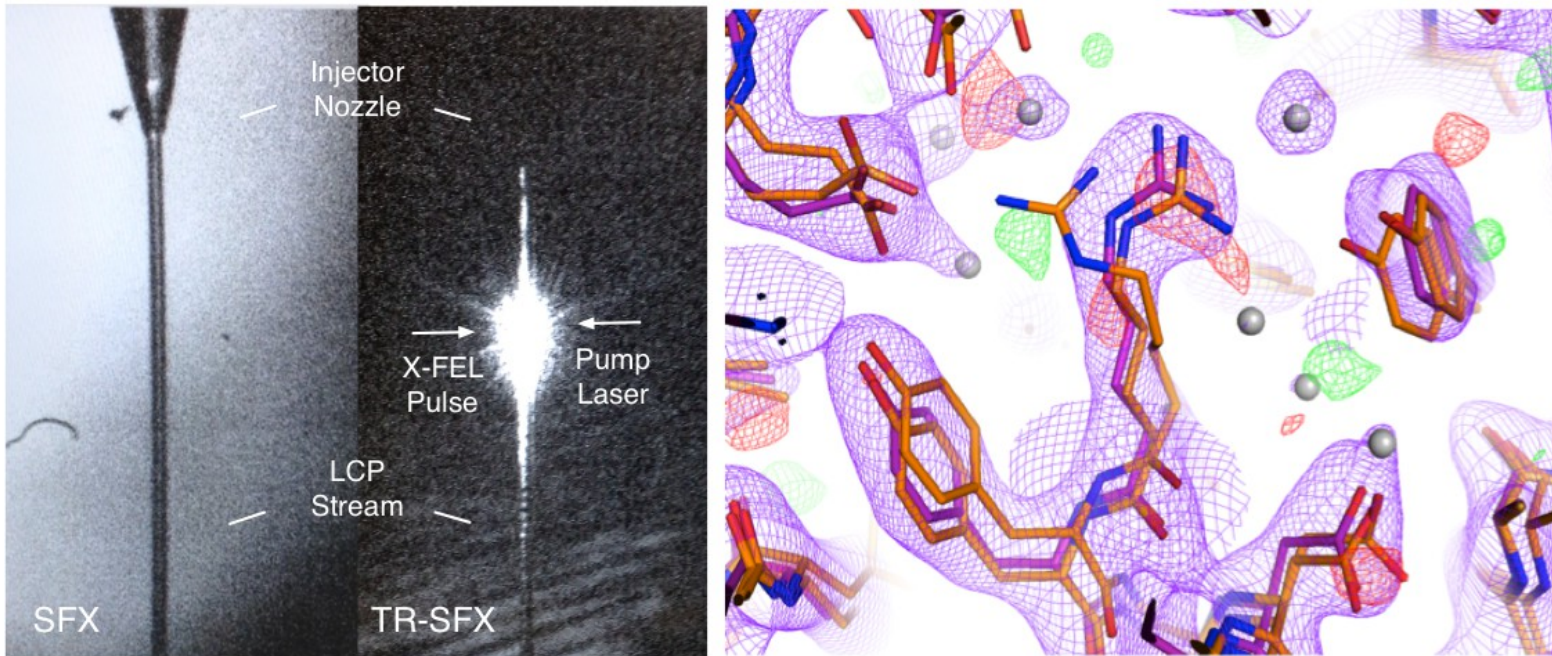
Fig. S5. (A) Approximate time course of concentrations of the intermediates in the PYP photocycle calculated from the mechanism show in the main text. Thick vertical lines: time-points in this study. (B) Real space correlation coefficients of DED maps from a time-series at 0°C (solid spheres) collected at BioCARS (Laue) versus the $1\ \mu\text{s}$ DED map from CXI (TR-SFX); positive DED features selected. Exponential rising and decaying phases are shown (solid line). Relaxation times are marked. Dotted vertical line: time-delay of the TR-SFX experiment at CXI.



Preliminary Time Resolved SFX-LCP data from LCLS

~ 40000 indexable patterns were collected in 12h of beamtime with 8000-10000 per time point

1 millisc time delay probes M1 state



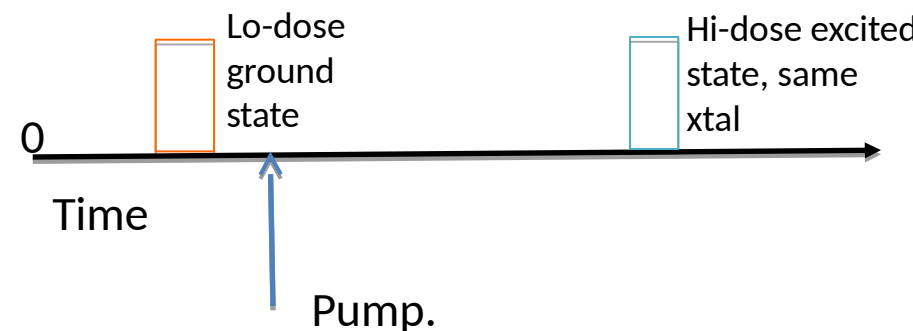
Fo-Fo difference maps at 3 sigma. Compatible with known conformational changes on bR activation for example a rotamer change of Arg82, a key residue in the proton transfer chain.

This is time-resolved (pump-probe) SFX at LCLS in LCP

For the future, BioXFEL will develop 2-color methods for SFX.



- Two successive hits from same xtal (first below damage threshold) with different wavelengths on the same camera readout. (Damage movie).
- * Pump pulse occurs between these.
- * No errors due to xtal size, orientation in difference
- * 2 Color also useful for SAD phasing (Wakatsuki)



Two-color patterns will improve TR-SFX accuracy.

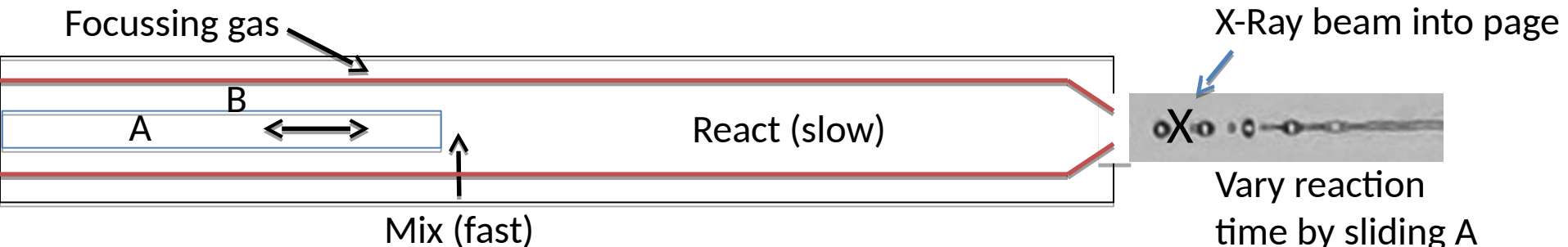
Chufeng Li PhD, Struct Dyn. Submitted
Submitted papers by Wakatsuki, Schlichting

Two-wavelengths from two successive pulses on same readout simulated for I_3C xtal ("Magic triangle").

BioXFEL is developing a mixing jet for dynamics

(eg. study of enzyme/substrate reactions, folding of DNA, tRNA)

D.Wang, J. Spence, U.Weierstall, L.Pollack J. Synch Rad. 2014.



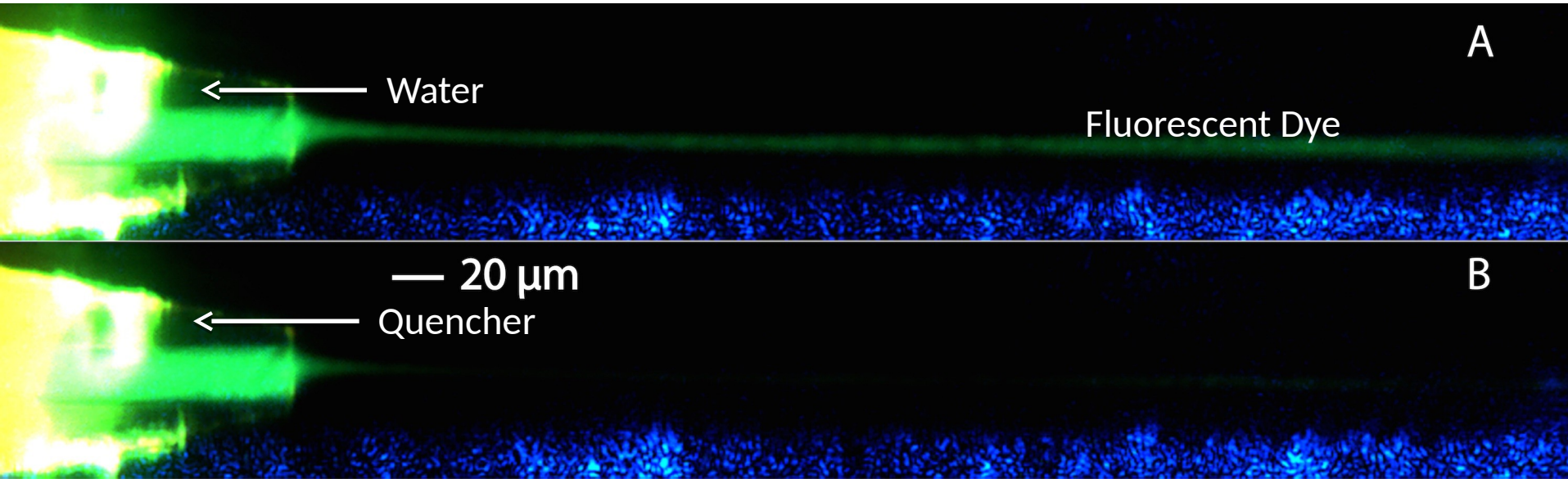
Mixing time (time resolution) is 200 - 300 microseconds

Reaction time adjustable from 200 microsec to 1 sec.

Diffusive mixing is possible using protein nanocrystals !

Outer flow rate 50 microliters/min. Inner flow rate 0.1 microliters/min.

Diffusion into nanocrystals is fast : 17 microsec for glucose into 0.5 micron crystal



Fast Solution Scattering (FSS)

Fluctuation cross correlations

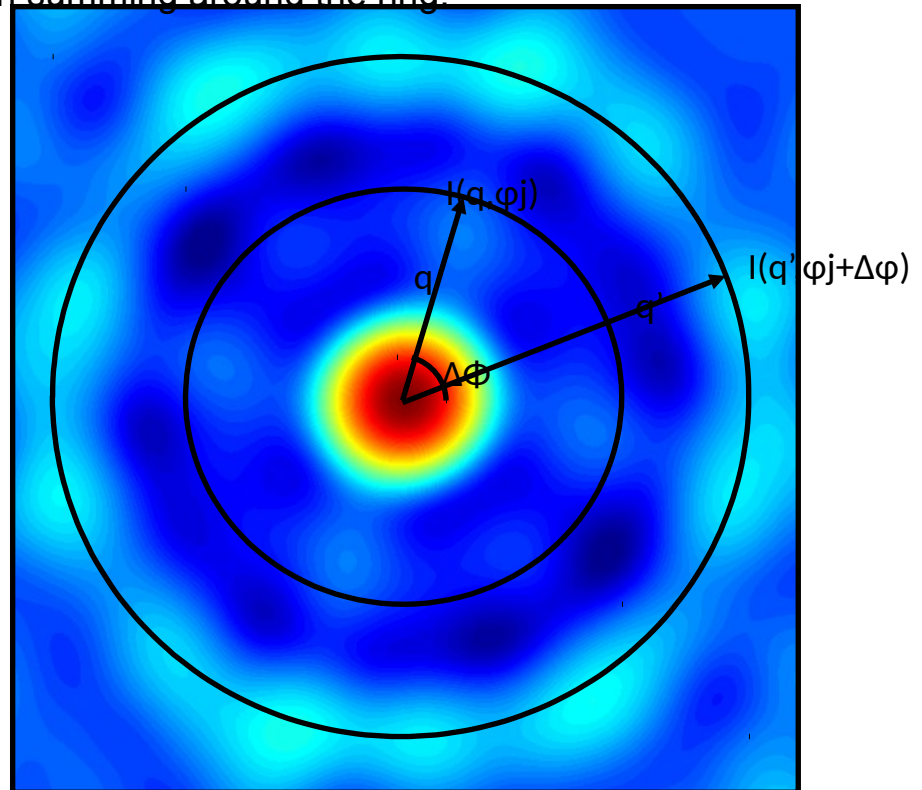
The experiment consists of detecting scattered intensity at TWO points on a ring, and multiplying these together. Then summing around the ring.

Averaged pair correlations are azimuthally symmetric, they depend only on $\Delta\phi$. We measure the angular cross correlation functions in the intensity *fluctuations*:

$$C_2(q, q', \Delta\phi) = \langle I'(q, \phi) I'(q', \phi + \Delta\phi) \rangle_\phi$$

$$I'(q, \phi) = I(q, \phi) - \langle I(q, \phi) \rangle_\phi$$

intensity fluctuation (mean subtracted ring intensity)



Donateli, Sethian, Zwart PNAS 2015 have new “one-step” phasing for Kam AC patterns. FSS is 2D for particles frozen in time time or space. Better inversion to 3D.

KAM's AC method for FSS has been demonstrated experimentally.

The image of one dumbbell has been reconstructed using XFEL snapshot scattering from randomly oriented dumbbells in solution.

Each diff pattern comes from *one particle per shot* in solution.
635 patterns.

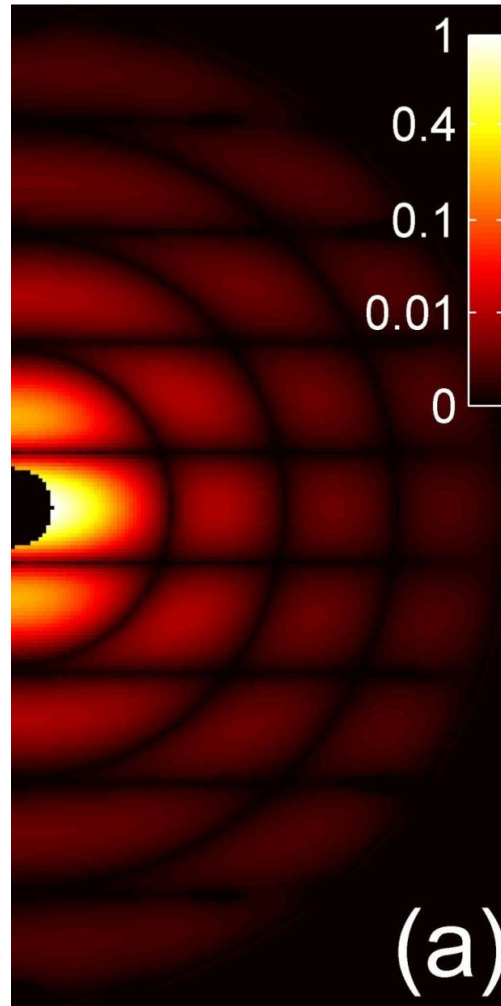
Two angles required to define orientation.

Ewald sphere curvature included
Cylindrical harmonic basis
Triple correlations from squared intensities used to get signs (phases)

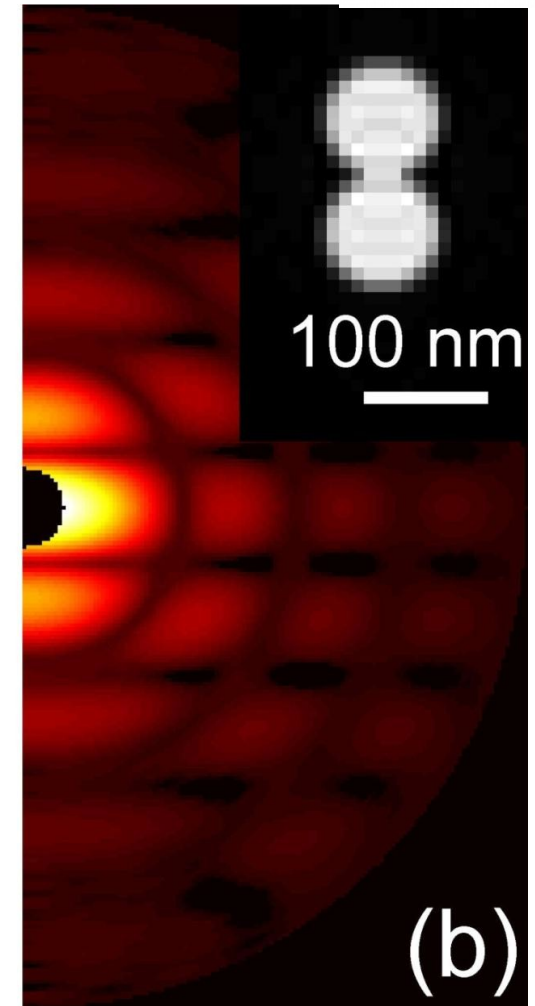
More recent (Pedrini) work had many particles per shot.

Polystyrene Dumbbells
Sphere diam 91 nm.
Resolution 10 nm.

Hit rate if many particles/shot
is 100% !!!!



Model



Experiment (one ptcle)

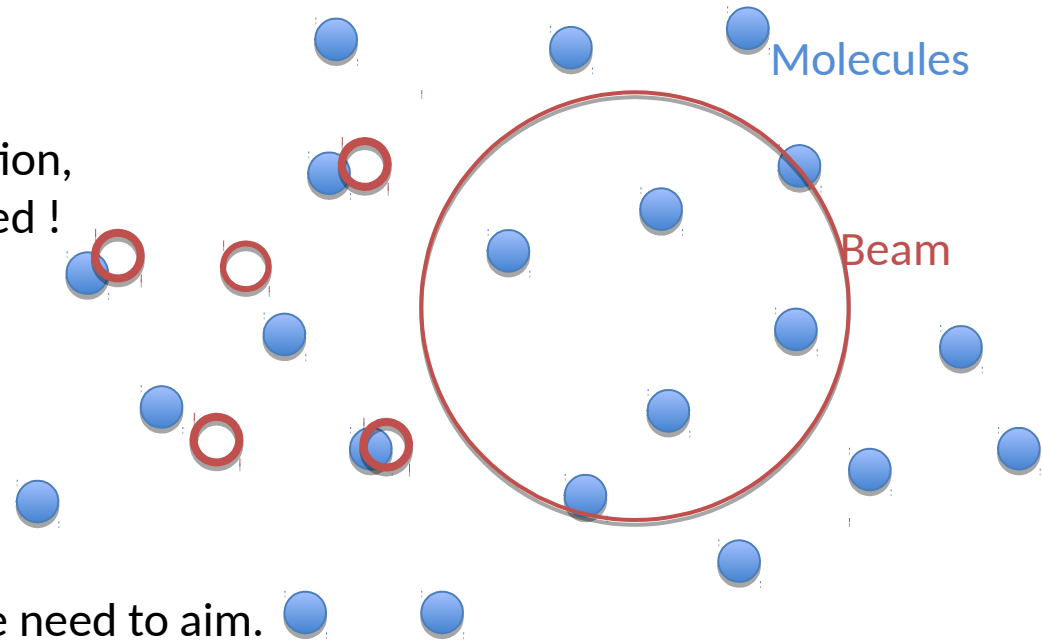
BioXFEL is developing the Angular Correlation (AC) method.

(This extracts image of one particle from scattering from many, randomly oriented)

Doubling FSS beam size gives same signal.
 FSS has 100% hit rate, avoids chamber vibration,
 beam position fluctuations. No aiming needed !

“Random hits with beam same size as ptcle
 give same signal/time as the same beam
 broadened over many particles”.

But targeted head-on SP hits are better,
 - less background more signal/time. Then we need to aim.



Pump-probe AC FSS difference method is most powerful

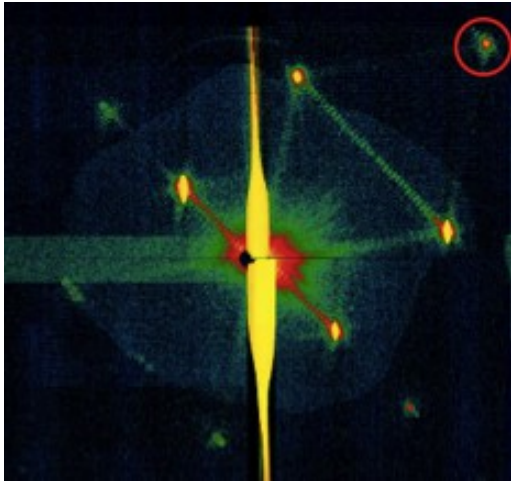
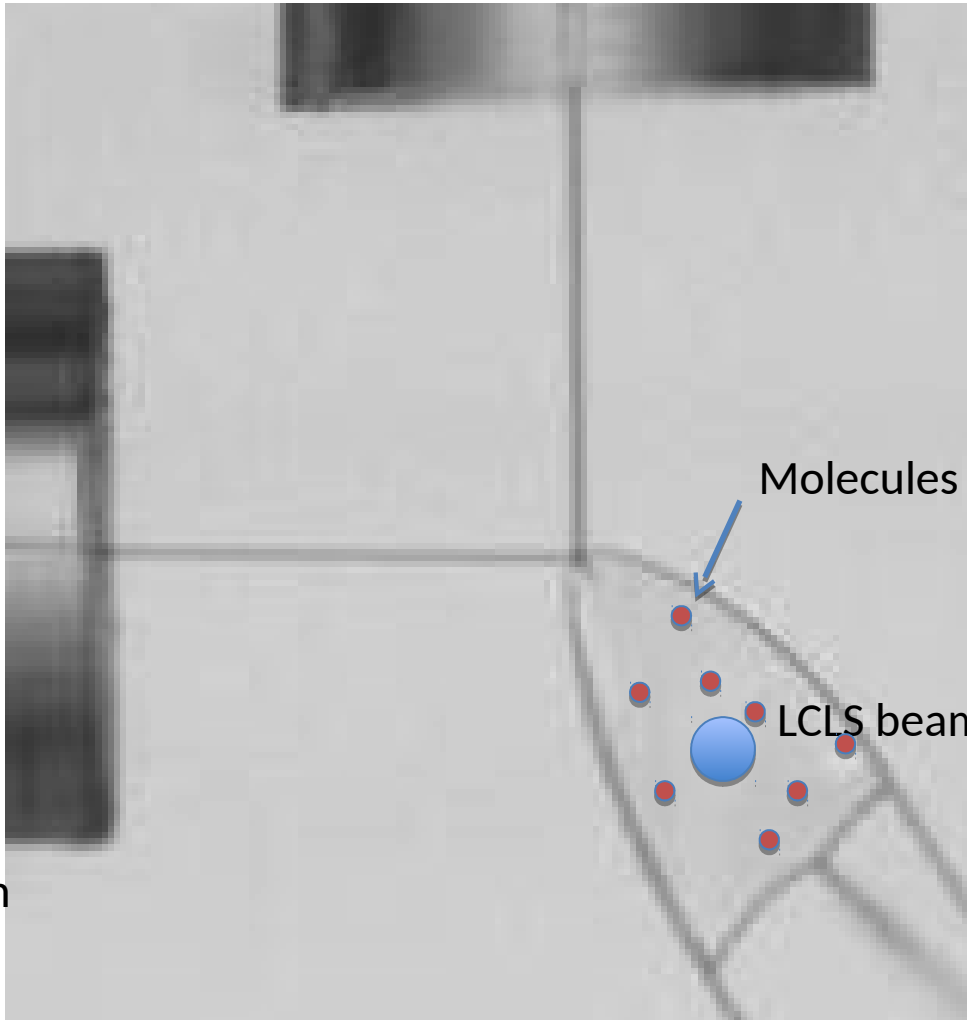
for structures known to high resolution by MX

We seek anisotropy in the Neutze FSS LCLS data set (Zwart , H. Liu, Spence).

Modelling can be combined with AC Kam method.

Sheet jets for FSS* to eliminate streak

*Fast solution scattering



Microliquids 2011

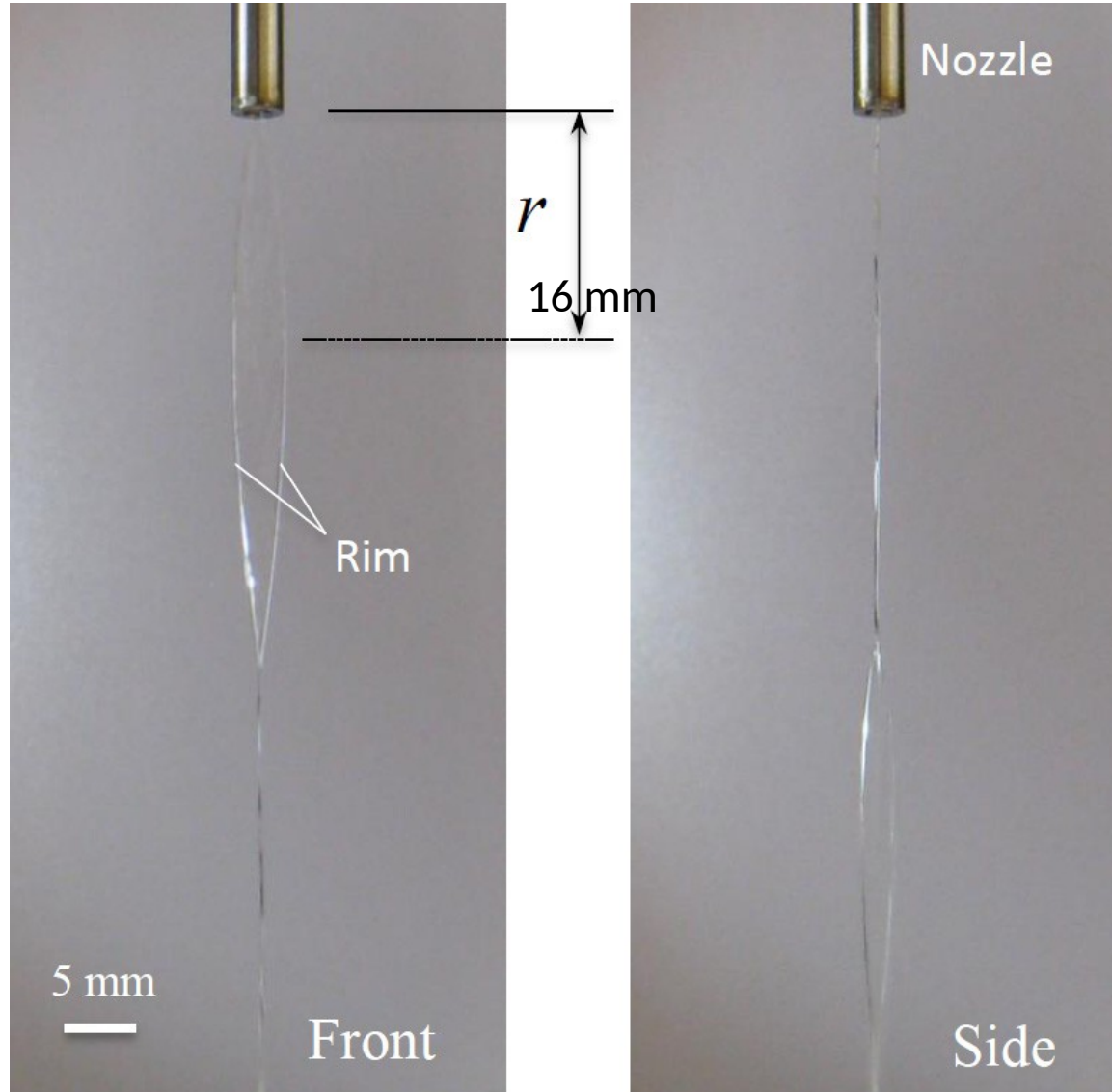
Fabricate using 2PP 3D printer with sub-micron resolution

Sheet jets would eliminate the diffraction streak from the jet for FSS

Experimental sheet jet running. We can use 3D printer to make these

Conc of mols
is low.
Thickness of
sheet 0.1 micron.

3D printed nozzles !

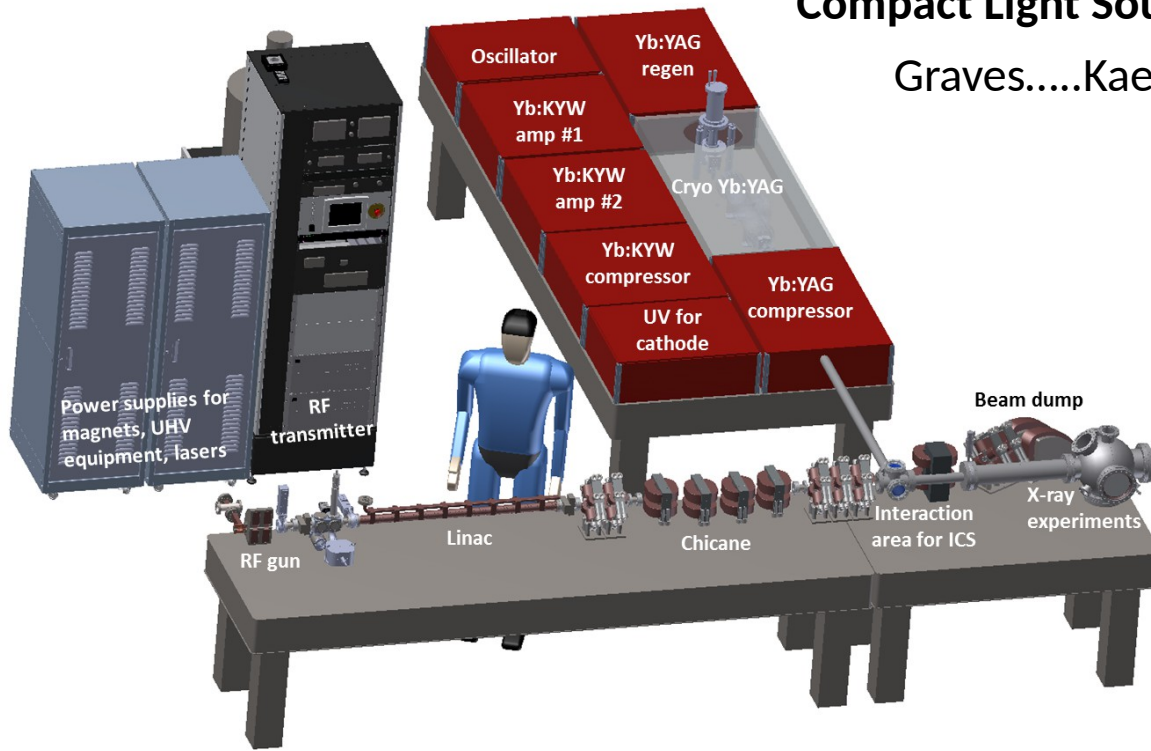


Ohba et al 2014
G.I. Taylor 1959
Savart 1833.

Fig. 3. Front- and side-view photographs of liquid sheet of water with flow rate of 130 mL/min. r : the distance from the nozzle exit.

Compact Light Source started at ASU (MIT design)

Graves.....Kaertner, Moncton. Phys Rev (2014)



Incoherent, phase 1

Linac + Inverse Compton.
Linac cavities fed separately
X-band. 18 MeV electrons
< 12 kV X-rays

Laser, phase 2

$$\lambda_x = \lambda_L / \gamma^2$$

Inverse Compton.
THz Linac.

Emittance exchange from
spatially patterned beam
for lasing.

FIG. 2: CAD layout of the components for the compact x-ray source showing the lasers including Yb:KYW that produces electrons via photoemission and the cryo Yb:YAG amplifier used for ICS. Accelerator components shown include the RF gun, short linac and transport magnets. The cabinets house the RF transmitter and power supplies for magnets, vacuum equipment, and lasers.

$$\lambda_x = \frac{\lambda_L}{4\gamma^2} (1 + a_0^2 + \gamma^2 \Delta\theta^2),$$

$$\left(\frac{d^2U}{d\omega d\Omega} \right)_e \approx \alpha h a_0^2 N_L^2 \gamma^2, \quad \text{for } N_L \text{ laser periods}$$

For SASE:

$$\frac{\Delta\lambda}{\lambda} = \frac{1}{N_u},$$

$$I = I_0 \exp\left(\frac{ut}{L_G}\right) = I_0 \exp\left(\frac{x}{L_G}\right).$$

If coherent, $I_x \sim N^2$

If incoherent $I_x \sim N$

$N_x \sim q V/\text{bunch}$

$$\lambda = \frac{L}{2\gamma^2} \left(1 + \frac{K^2}{2} \right),$$

$$L_G = \text{constant} \times \left(\frac{i}{\Sigma} \right)^{-1/3} B_0^{-2/3} L^{-1/3} \gamma,$$

Σ - bunch cross section
N e- per bunch.

Summary of 12 keV parameters

(incoherent ICS, undulator-like radiation)

Parameter	0.1% Bandwidth	5% Bandwidth	Units
Average flux	2×10^{10}	5×10^{11}	photons/s
Average brilliance	7×10^{12}	2×10^{12}	photons/(s .1% mm ² mrad ²)
Peak brilliance	3×10^{19}	9×10^{18}	photons/(s .1% mm ² mrad ²)
RMS horizontal size	2.4	2.5	microns
RMS vertical size	1.8	1.9	microns
RMS horizontal angle	3.3	4.3	mrad
RMS vertical angle	3.3	4.3	mrad
Photons per pulse	2×10^5	5×10^6	
RMS pulse length	490	490	fs
Repetition rate	100	100	kHz

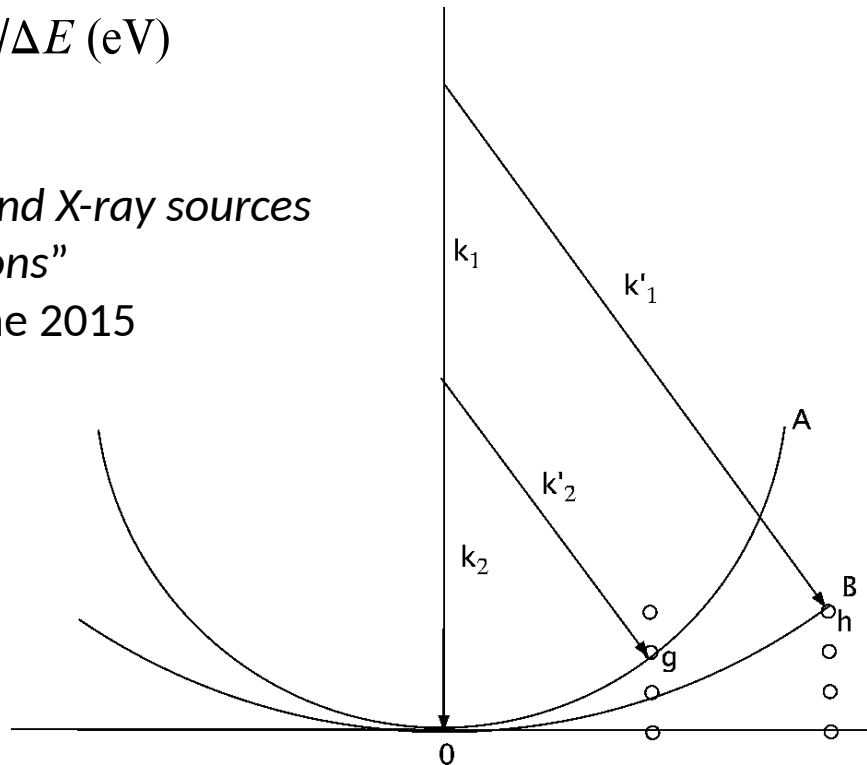
Compact incoherent source for ASU, not lasing. Graves et al Phys Rev 2014

Lasing achieved later by patterning the beam, emittance exchange, Short THz linac (Graves et al Conf. 2014).

Attosecond XFEL avoids damage, gives full Braggs, not partials.

$$\Delta t \text{ (fs)} = 4.14/\Delta E \text{ (eV)}$$

“Compact attosecond X-ray sources and their applications”
Workshop CFEL June 2015



Different wavelengths cause different Bragg reflections to interfere on same detector pixel, if pulse duration less than beat period. This gives structure factor phase information.

Attosecond XFEL gives 300 eV = 3% bandwidth at 10 kV with 14 as pulses, hence full reflections, without damage.

Coherence length $L = \lambda E/\Delta E \sim 3\text{nm}$, less than sample thickness !

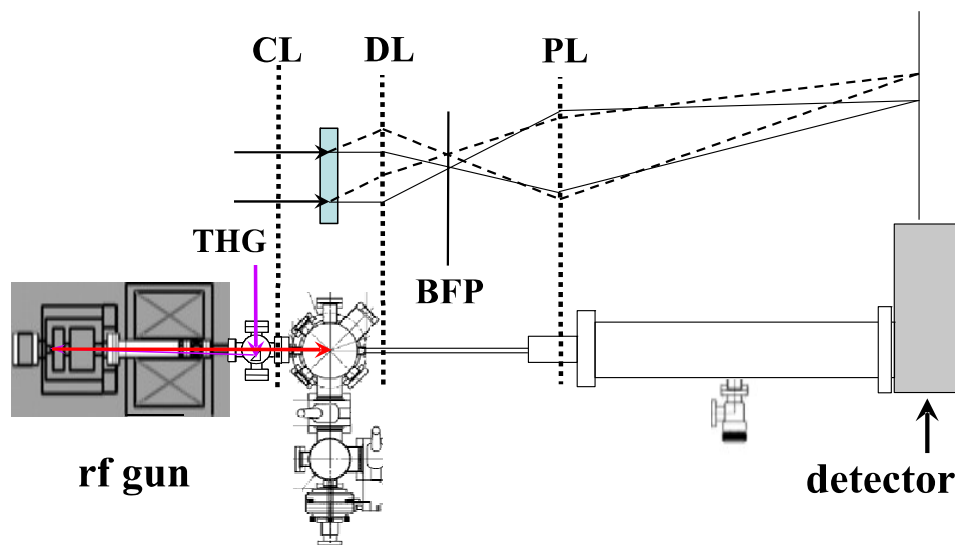
3-phase sums (as above, plus Friedel conjugate of sum) are origin independent.

Can electron beams outrun radiation damage ?

When focusing a 500 micron diameter beam on an approximately 0.1 micron "virus" we find less than one electron scattered per 100 fs shot. (3MeV, Murooka's system).

Or 49,043 elastically scattered electrons if beam could be focused down to 0.1 microns.

Cryo-em "dose"
is about $10 \text{ e}^-/\text{Ang}^2$



Electron Diffraction Camera. 3 MeV, $1.06\text{E}6 \text{ e}^-/\text{pulse}$, 100 fs, 500 μ beam
Murooka et al 2011.

Electrons which loose energy continue to detector to make background, unlike X-rays !

Spence, Musumeci, Subramanian, "Applied Physics" 2015. submitted.

“Hollow cone” allows *large incoherent* source for fast e⁻ imaging at hi-res.

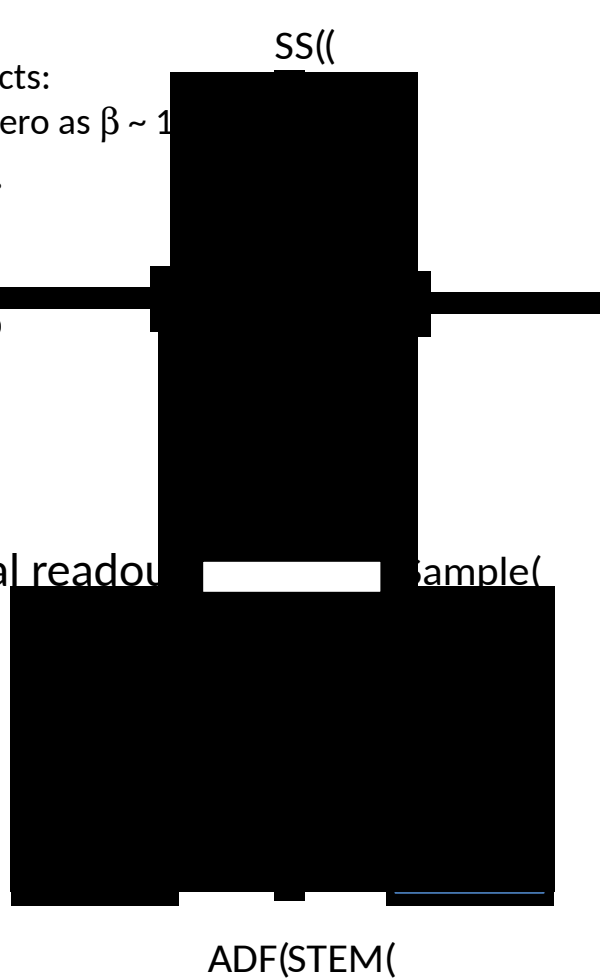
Atomic-resolution imaging does **not** require coherent illumination, which wastes electrons.

Space-charge effects:

Lorentz force to zero as $\beta \sim 1$

1. One e-/shot .
2. Dark field.
3. High energy
4. Spherical cap

Scan for serial readout of image of sample



ADF(STEM(



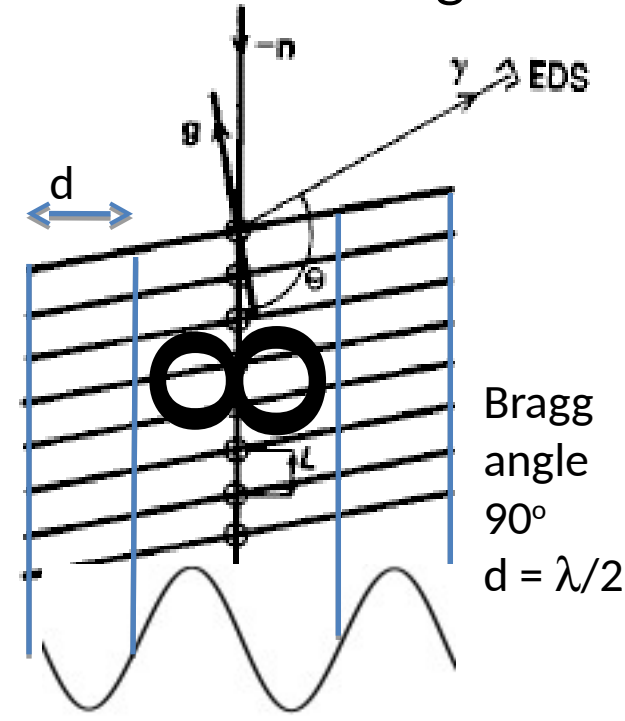
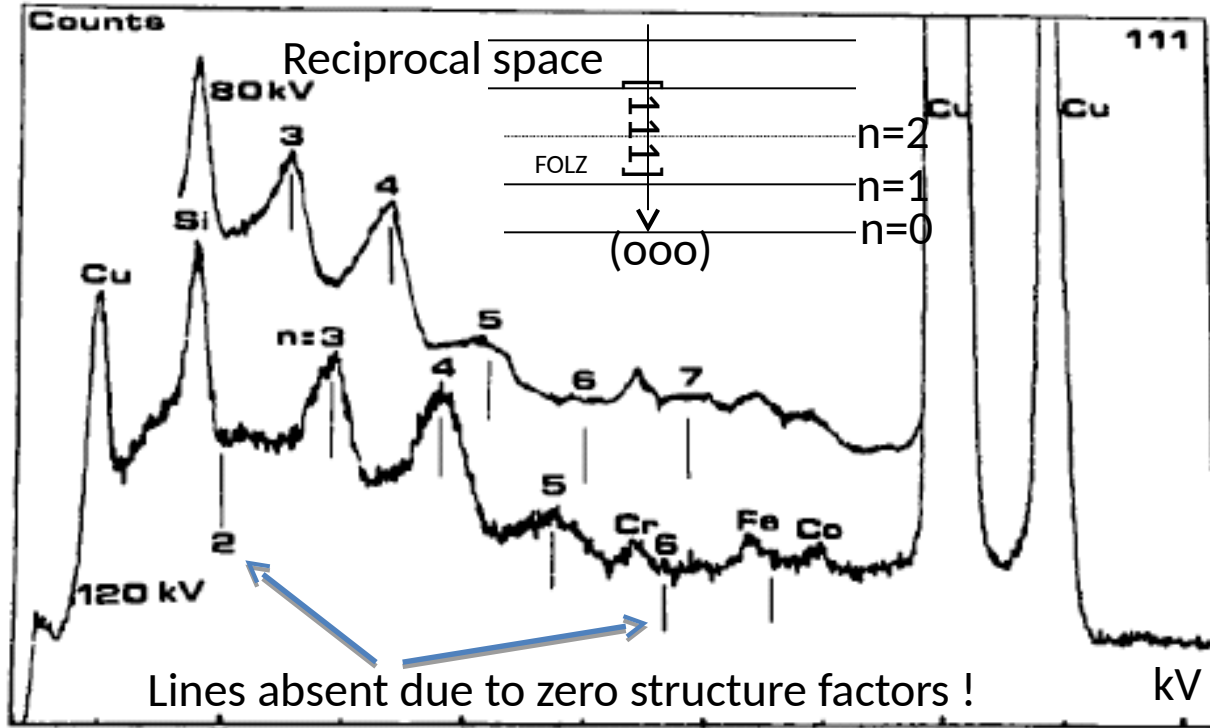
Hollow(cone)TEM(

Spence et al, Applied Physics 2015. submtd

Full-field image simultaneous in every pixel (camera)

1. Under reciprocal apertureing conditions (identical objective lenses) the STEM scanned image is identical to that produced immediately at every pixel in the TEM.
2. *The number of electrons arriving per unit time at every pixel of the HC-TEM image is the same as that arriving at the whole STEM detector, for one STEM probe position, if the brightness of the extended HC source is equal to the STEM point source. (may be reduced by*

Crystal undulators for lasing using Coherent bremsstrahlung



Frequency at which beam e^- encounters atoms in its path is $\omega = 2 \pi v / L = 2 \pi c \beta / L$

$$E = 12.4 \beta / L(1 - \cos \theta)$$

Continuous Brem from glassy target concentrates into lines for xtal, one for each extinction dist.

Harmonics may be labelled with Miller indices for layer of reciprocal lattice points responsible

The NSF BioXFEL STC Research Consortium

Biologists

University@Buffalo HWI
E. Lattman, E. Snell, T. Grant*
 Outreach, nanocrystals, data

ASU
J. Spence, Zatsepin*
 Science, Data analysis

**Techniques
 (Methods Group)**

established Oct 2013

U. Wisc. Milwaukee
M. Schmidt
 Energetics of Bioreactions

Center for Applied
 Structural Discovery
 (CASD) ASU

Rice
G. Phillips:
 conformational variability

UCSF
R. Stroud
 membrane proteins

BioXFEL
 STC

ASU
P. Fromme:
 membrane proteins
B. Hogue: viruses

Stanford
R. Kornberg
 D. Bushnell: Pol II, S.P.
 transcription complex

Puerto Rico International conference,
 Data Analysis Workshop,
 LCP injector sales (17), Beamtimes, LCLS 2.
 Crystallization workshops at HWI.

Cornell
L. Pollack:
 mixing reactions

LBL, LLNL
 Unfunded collaboration
J. Holton, M. Frank, S. Hau-Riege

U. Wisc. Milwaukee
A. Ourmazd, D. Saldin:
 SP data analysis

ASU
 injectors
**Weierstall,
 Kirian**

DESY
 Unfunded collaboration
Chapman, Messerschmidt*

Current BioXFEL work includes...

- 1. GPCRs for drug design. Cherezov, Weierstall, Stevens collab.**
- 2. Beyond Monte Carlo - optimization and partiality. White, Li, Zatspin.**
- 3. Time-resolved SFX for photosynthesis. Schmidt, Fromme.**
- 4. Fast Solution Scattering (FSS). Mixing jet, Kam method, Angular correlations.**
- 5. Viscous jets. LCP with XFEL or SR, in helium, Agarose for solubles.**

**Building blocks have explanatory power for understanding mechanisms in matter.
eg The α -helix in bio - need only 6 Ang resolution to see it.**

- Atoms at 2 Ang for mat sci., cond matter. Eg kink landscape.

**Current XFELs need Bragg Boost (& lasing) to see them (or modelling, Bayesian)
So either learn to make 10x10x10 xtals or build 1E6 times more powerful XFEL.**

**TR-SFX in Bio can image molecular machines inside one molecule in one hydrated
unit cell (hence get Bragg boost), not possible in a continuously bonded silicon wafer**

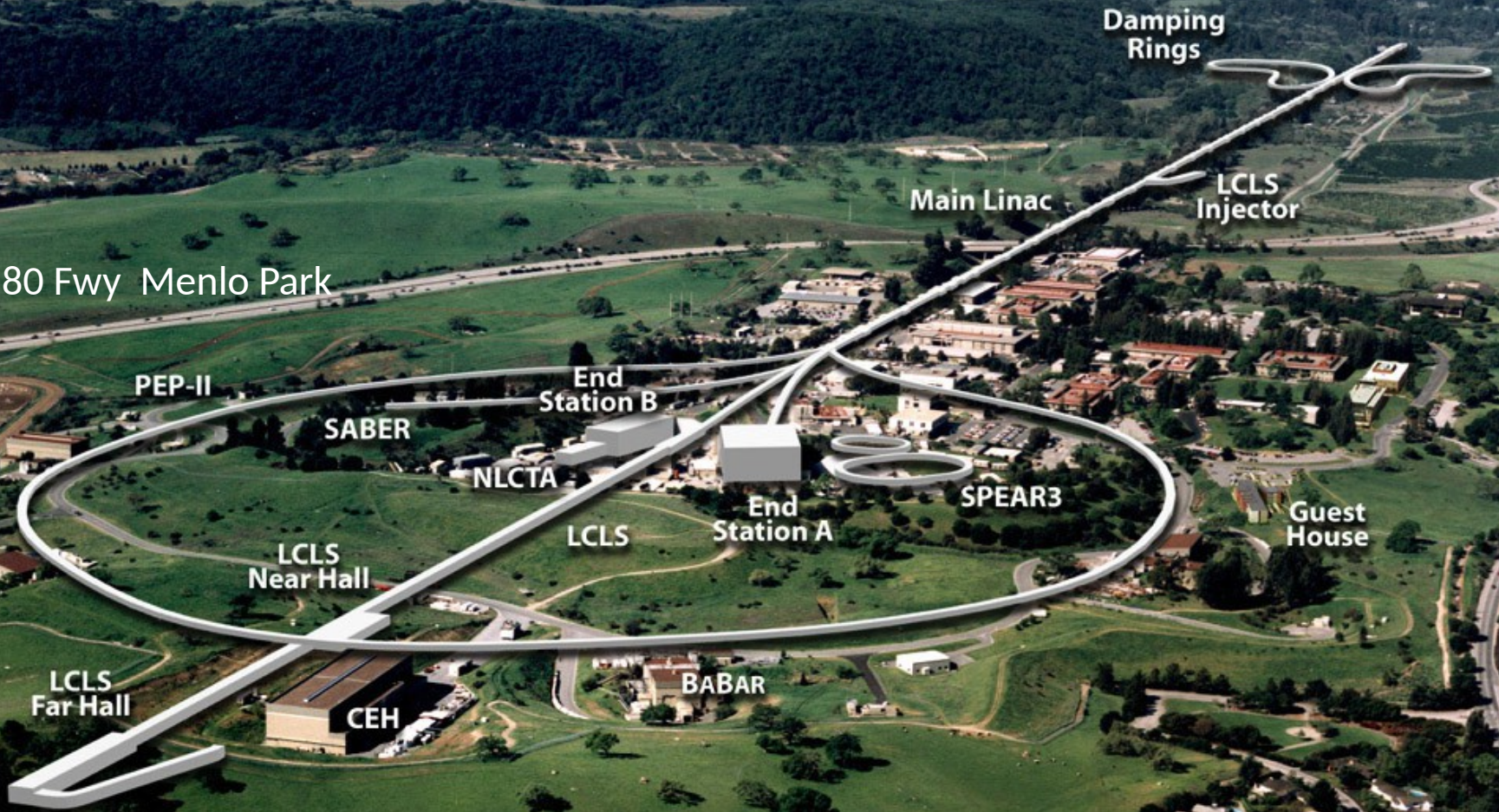
**The transition from SP (one ptcle per shot, needs aiming) to a few per shot (no
aiming) is continuous.**

Exciting times ahead !

The End

The birth of a new field

280 Fwy Menlo Park



With thanks for many collaborators from CFEL, MPI, ASU, SLAC, Uppsala.

The last fifteen years has seen two important breakthroughs in imaging science :
Lensless imaging and outrunning damage..



"Physics is a problem in search of a solution; Biology a solution in search of a problem".

"The successful man adapts himself to the world, the failure tries to change it.
Therefore all progress depends on losers". GBS